General Disclaimer

One or more of the Following Statements may affect this Document

- This document has been reproduced from the best copy furnished by the organizational source. It is being released in the interest of making available as much information as possible.

- This document may contain data, which exceeds the sheet parameters. It was furnished in this condition by the organizational source and is the best copy available.

- This document may contain tone-on-tone or color graphs, charts and/or pictures, which have been reproduced in black and white.

- This document is paginated as submitted by the original source.

- Portions of this document are not fully legible due to the historical nature of some of the material. However, it is the best reproduction available from the original submission.

NASA CR- 145373

(NASA-CR-145373) SIGNATURE ANALYSIS OF ACOUSTIC EMISSIONS FROM COMPOSITES Final Report, 1 Oct. 1975 - 30 Mar. 1978 (Virginia Polytechnic Inst. and State Univ.) 79 p HC A05/MF A01 CSCL 11D G3/24

N78-23148

Unclas 16744

COLLEGE OF ENGINEERING

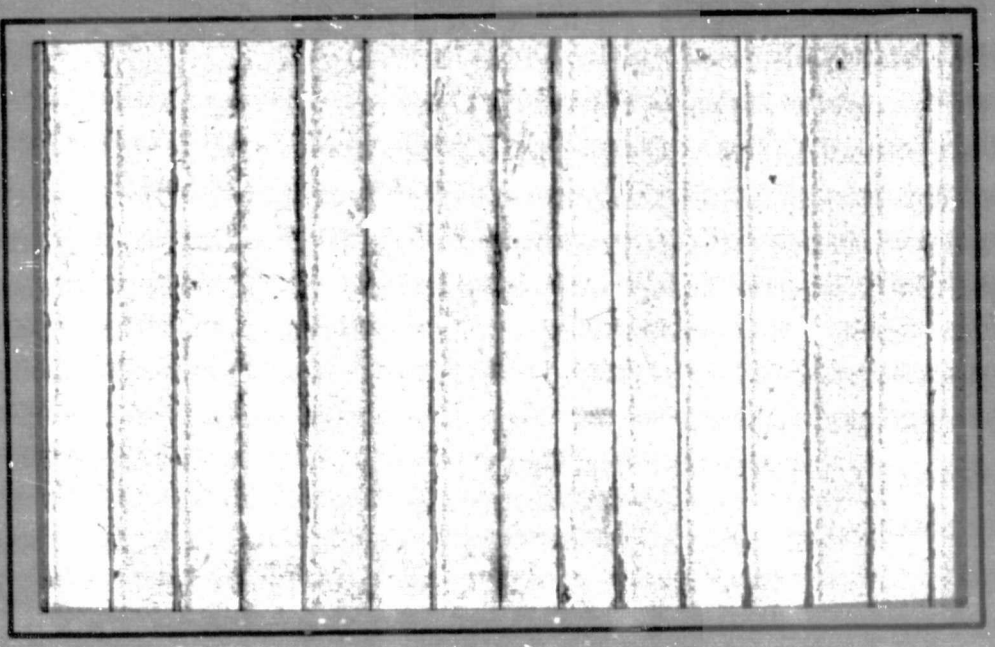

VIRGINIA POLYTECHNIC INSTITUTE AND STATE UNIVERSITY

BLACKSBURG, VIRGINIA

SIGNATURE ANALYSIS OF ACOUSTIC EMISSIONS FROM COMPOSITES

NASA Grant NSG 1238

Final Report for the period
October 1, 1975 - March 30, 1978

by

Edmund G. Henneke, II
Associate Professor
Department of Engineering Science and Mechanics
Virginia Polytechnic Institute & State University
Blacksburg, Virginia 24061

The NASA Technical Officer for
this grant is Gregory R. Wichorek
NASA-Langley Research Center
Hampton, Virginia

BIBLIOGRAPHIC DATA SHEET	1. Report No. NASA CR-145373	2.	3. Recipient's Accession No.

4. Title and Subtitle

SIGNATURE ANALYSIS OF ACOUSTIC EMISSIONS FROM COMPOSITES

5. Report Date: May 19, 1978

6.

7. Author(s): Edmund G. Henneke,II

8. Performing Organization Rept. No.

9. Performing Organization Name and Address

Virginia Polytechnic Institute & State University
Engineering Science and Mechanics Dept.
Blacksburg, Virginia 24061

10. Project/Task/Work Unit No.

11. Contract/Grant No.: NSG 1238

12. Sponsoring Organization Name and Address

NASA-Langley Research Center
Hampton, Virginia

13. Type of Report & Period Covered: Final Report 10-1-75 thru 3-30-78

14.

15. Supplementary Notes

16. Abstracts

See attached

17. Key Words and Document Analysis. 17a. Descriptors

Composites, Acoustic Emission, Time Signatures, Signal Analysis, Frequency Spectra, Graphite-epoxy

17b. Identifiers/Open-Ended Terms

17c. COSATI Field/Group

18. Availability Statement	19. Security Class (This Report) UNCLASSIFIED	21. No. of Pages
	20. Security Class (This Page) UNCLASSIFIED	22. Price

TABLE OF CONTENTS

ABSTRACT

Acoustic emission data were obtained from a series of tensile tests on specially designed graphite-epoxy unidirectional laminates. The design was such that the specimens would preferentially fail first by fiber breakage and later by matrix splitting. The AE signals for each of these events have been analyzed and some typical results are reported herein. Patterns characteristic of each failure mechanism have been noted for both the time signatures and the corresponding frequency spectra.

LIST OF FIGURES

Page

1. INTRODUCTION

Everyone who has performed a mechanical test on a composite material is well aware of the audible noises that emanate from the specimen at loads ranging from intermediate to failure. Because of this noisy evidence of damage processes occurring prior to failure, it has been natural for interest to develop in using these acoustic emissions as a means for studying the early nucleation and progression of damage in composites. Much fundamental work needs to be performed, however, before useful, definitive information can be gleaned from the acoustic emission signals. It was the purpose of the work to be discussed in this final report to initiate one such basic study. The objectives of this work were (1) to determine if various composite failure modes are distinguishable by signature analyses in specimens for which the failure modes can be visually observed, (2) to delineate what type of signature analysis is the most appropriate for the study of failure modes, (3) to determine if the experimental data obtained in these basic studies can be extended to more complex composite structures such as laminates, and (4) to develop an experimental technique which could be used not only for laboratory research purposes but which could be modified for field use.

During the two and one-half years this grant has been in force, work has been performed on the first three objectives, with particular emphasis being placed on the first two. Obviously it is necessary to obtain answers to these two objectives first before meaningful approaches can be taken towards finding solutions for the last two objectives. It does now appear likely that the specific two failure modes, fiber breakage and longitudinal matrix splitting, can be distinguished by appropriate signature analysis. However, it must be emphasized here that it is still not possible to state

this as a definitive conclusion from the present work. While all possible care was taken in performing the experiments, and as simple a laminate as possible was chosen for study, specimen and experimental variables were such that it was not always possible to definitely identify a particular acoustic emission with a particular observed failure mode event. Two distinctive signature patterns have been identified for the unidirectional graphite-epoxy laminates used here that were more often than not correlated, respectively, to the two fracture modes. However, there were instances where one or the other of the signature patterns were observed together with a visual observation of the "wrong" failure mode for that pattern. It is possible, and highly likely, that the two failure modes were acting simultaneously, or nearly so, and that the visual observation technique used did not have the resolution required to separate the two. This fact, together with the rapid occurrence of several acoustic emissions, could account for the sometime opposite correlation of signature pattern and failure mode. It is because of this that a more definitive conclusion should not be made at the present time from this work.

In the sections that follow a short review is given of work performed under this grant that has been more thoroughly discussed in other, earlier reports, and that has been accomplished since the last reporting period.

2. REVIEW OF PREVIOUS WORK PERFORMED UNDER GRANT

2.0 Background

Work performed during the first two years of the grant period has been discussed in four previous reports [1-4]. Reference [4] is an Interim Report which summarizes all the work performed during the first two years and which is based upon the Master's Thesis of S. S. Russell [5]. Mr. Russell was supported during his entire stay at Virginia Tech by this grant. For completeness of the present, final report, this section gives a synopsis of this earlier work.

2.1 Experimental Methods

The specimens chosen for study were three-ply, unidirectional graphite-epoxy tensile coupons. These coupons were made with a gap of approximately one-quarter inch in the outer plies in the center of the gauge length. That is, only the center ply ran the entire length of the specimen. A notch was started in this gapped section by pricking the middle ply with a knife. This specimen failed by the crack extending across fibers for one-eighth to one-quarter inch before stopping and then later cracking parallel to the fiber direction exclusively in the matrix. Several other simple specimen geometries were investigated [4], but none of these others had a reproducible sequence of distinct failure modes as did these three-ply specimens. These specimens provided another advantage. It is experimentally difficult to obtain the transfer function for the specimen-transducer instrumentation system. In fact, the transfer function will change as the specimen is loaded. Thus an exact picture of the acoustic emission signature is not obtainable. However, if two different failures that are closely spaced in time and in terms of

damage to the specimen are analyzed, the effect of being viewed through a different specimen response function is minimized. By comparing two closely spaced emissions, qualitative trends may be noted. The three ply $[0_3]$ specimen with one-quarter inch gap provided the two types of closely spaced emissions required.

These specimens were subjected to quasi-static tension loading on an Instron Model 1125 test machine at a crosshead rate of .01 to .05 in/min, depending on the test. An optical microscope mounted on a stage attached to the crosshead, and later a television camera with a close-focus lens, was used to observe the growth of a crack from a damaged region. The transducers used to monitor the acoustic emissions were a Panametrics 5070AE-0 cross-coupled, 1/4" x 1/4" unhoused transducer and an Acoustic Emission Technology, Model FAC 500 housed transducer, 1" diameter. Both transducers were bonded to the specimen with double sided sticky tape and held in place by masking tape.

The signal was transmitted from the transducer to a Panametrics ultrasonic preamplifier, then to a Tektronix Type 1A7A differential amplifier, and was recorded on a Honeywell 5600B tape recorder at 60ips [Fig. 1]. The dynamic response and amplification of the electrical equipment is discussed below. The settings of 40 dB on the preamplifier and .2 Volts/cm on the Type 1A7A differential amplifier were experimentally determined to be best suited to keep the signal significantly large in amplitude without saturating the tape recorder amplifier. The band width selector on the differential amplifier was set to pass frequencies between 100 Hz and 300 KHz. This setting reduced low frequency noise and insured no Nyquist-related problems existed. On a parallel track on the tape recorder, voice comments on the test were recorded. An oscilloscope was also connected to visually monitor the emissions.

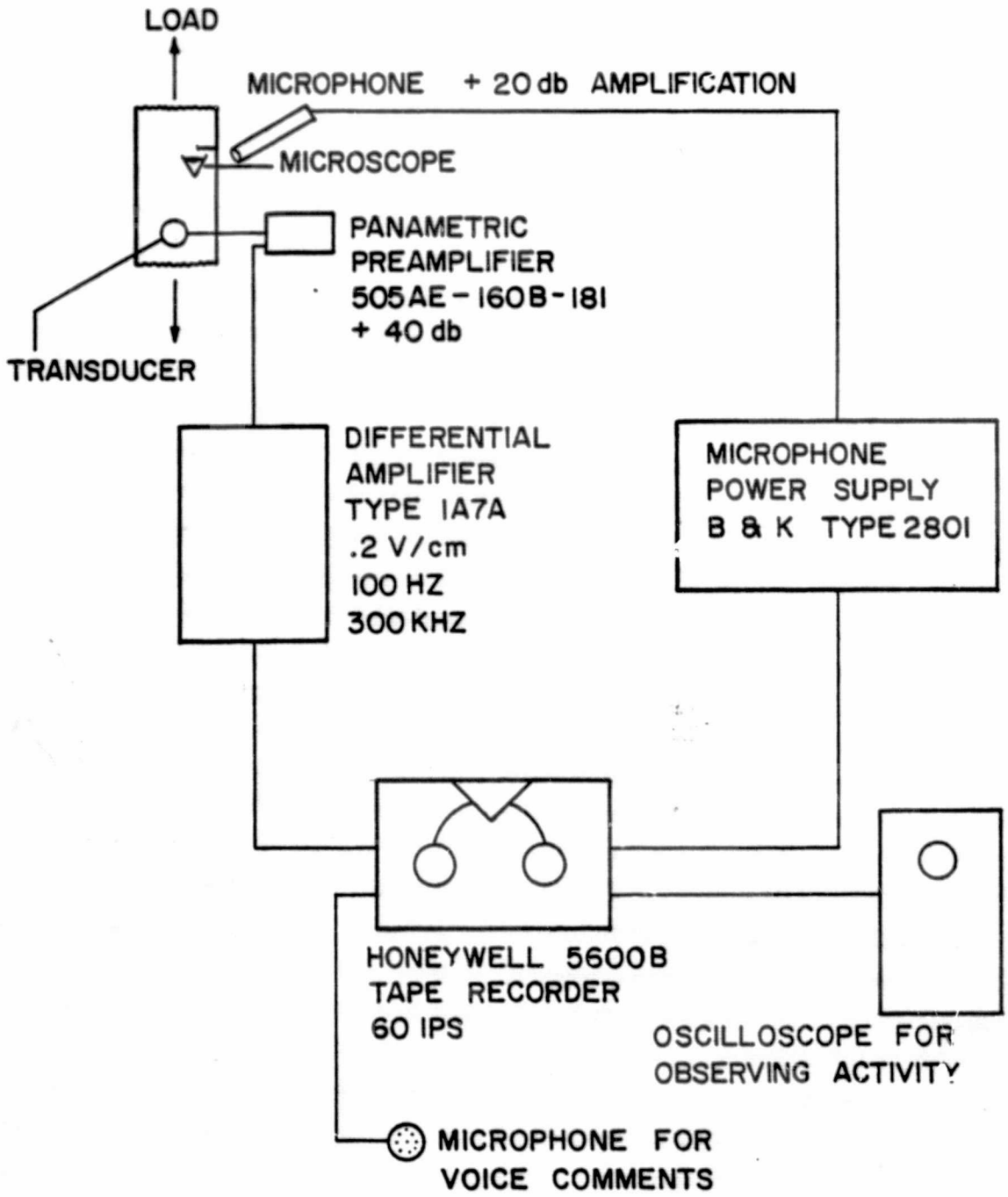

Figure 1. Electrical Equipment for Recording Acustic Emissions

After a series of tests were performed the acoustic emissions were digitized by a Biomation 805 waveform recorder that was interfaced to a microprocessor unit (CB**2) [6] [Fig. 2]. The digitizing interval used was usually .2 microsec/point. Since there are 2048 points of storage available on the recorder this resulted in a signal 409.4 microsec. in duration. The digitized signal was stored on the microprocessor's tape unit. When a group of signals were on the tape unit, the microprocessor was interfaced with the central IBM 370 and the signals were transmitted to storage in the IBM 370 and punched on cards for later analysis by a computer program.

An attempt was made to determine the frequency response of the acoustic emission transducer and the instrumentation system. For the latter, a sine wave of known frequency and amplitude was introduced into the input of the Panametrics preamplifier as a simulated emission. Signal analysis was performed on the resulting recorded signal as if it had been an acoustic emission. This test indicated an approximately flat frequency response for the instrumentation system between 30 KHz and 300 KHz with a system gain of 45 dB. Tests then ran on the acoustic emission transducer indicated that the FAC 500 transducer has a response curve which, although not flat, is free from very sharp resonances [Fig. 3].

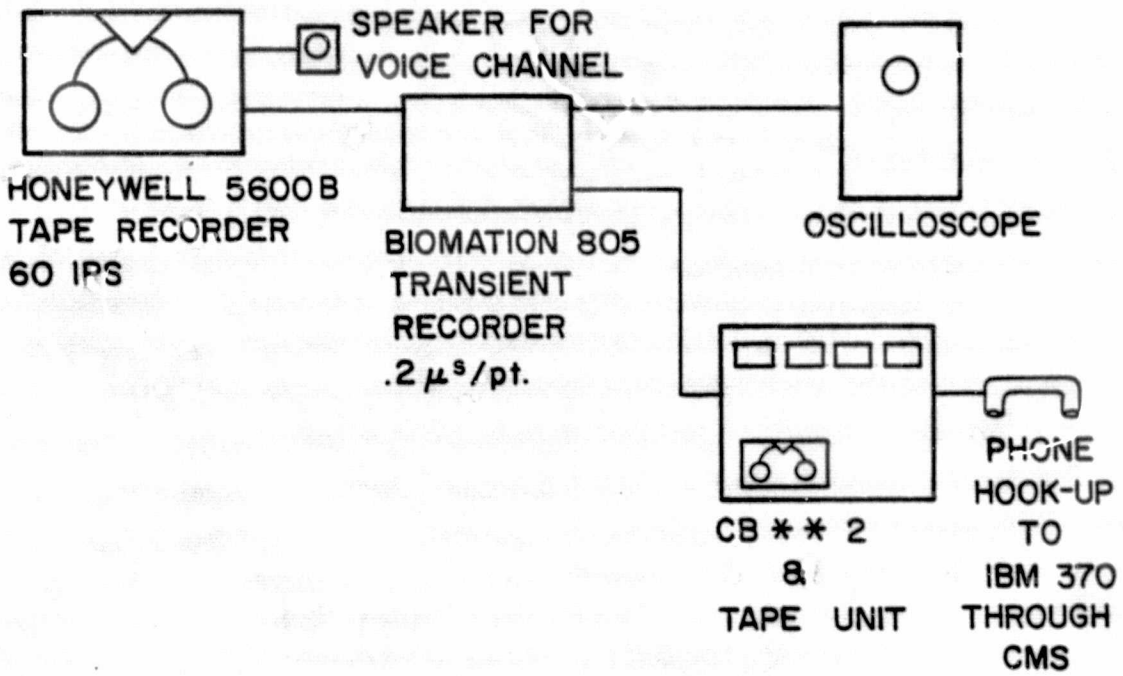

Figure 2. Electrical Equipment for Selecting, Digitizing, and Transmitting Data to Computer

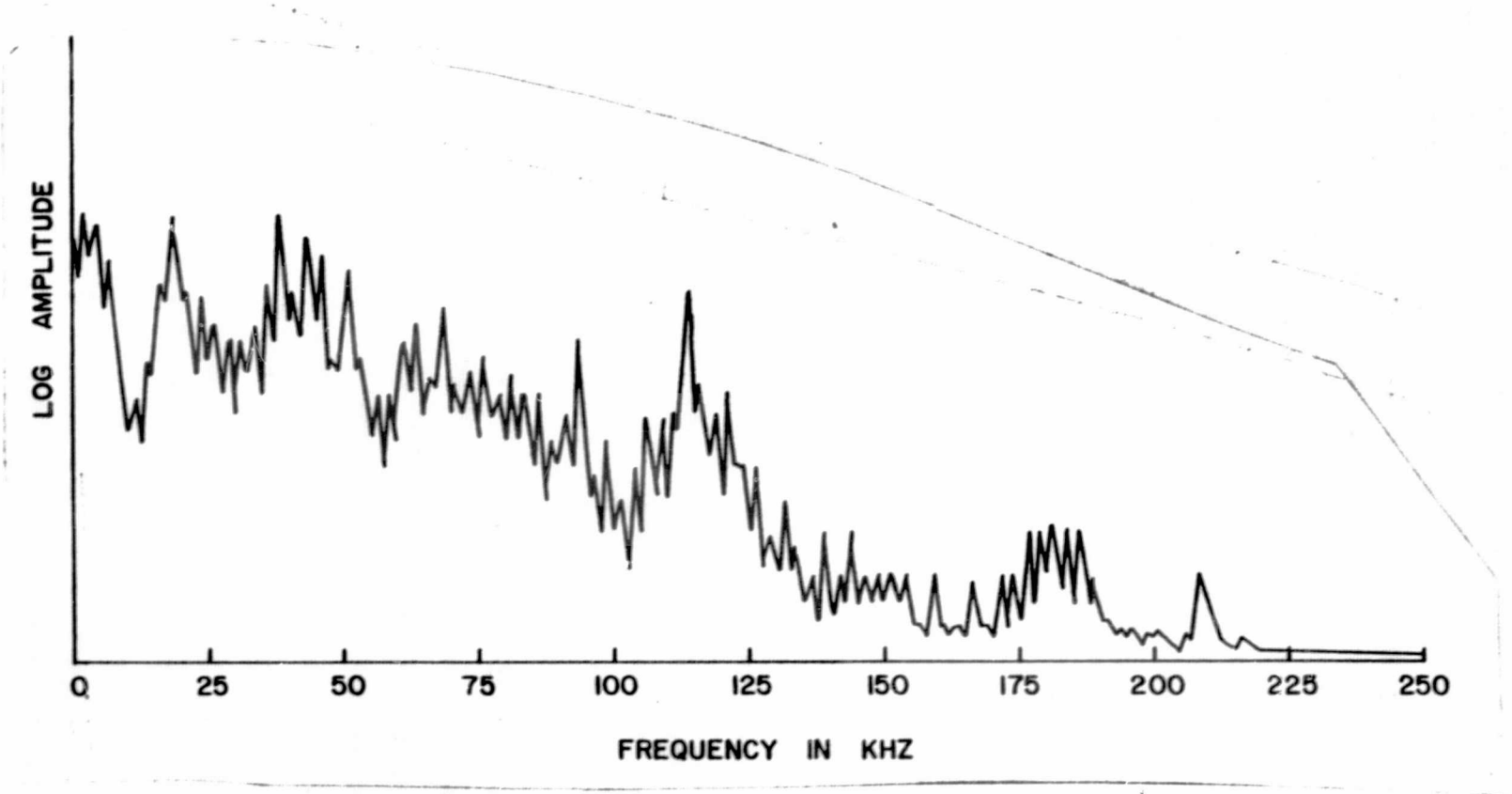

Figure 3. Frequency Response of FAC500 Transducer using Coarse Sandpaper for Excitation

2.2 Results

During the course of the experimental work many $[0_3]$ specimens, with the center ply being the only continuous ply, were tested with different gauge lengths. It was hoped that by varying only the length the vibration characteristics of the specimens would be changed, and, therefore, the frequency analysis of the acoustic emissions would change except for possibly some detail that would remain constant and hence be characteristic of the failure mode being studied. This line of study was unproductive in revealing the characteristic details of emissions from various types of failure. However, when a comparison of several acoustic emissions from the same specimen is made some patterns are apparent. Typical examples of the results obtained are presented in Fig. 4-7.

Figure 4 presents the time signature of an acoustic emission event caused by the transverse propagation of edge notch, i.e., a failure event involving the fracture of some graphite fibers. This emission was very energetic, having a maximum amplitude of 4.3 volts as recorded on the tape recorder (24.2 mv signal at the source). As can be seen in Fig. 4, this emission required more than 80 μsec for the amplitude to rise to the maximum peak and decayed very slowly. Figure 5 is the frequency transform of the time signature shown in Fig. 4. The acoustic emission transducer appears to respond to frequencies only between 20 and 110 KHz, filtering out all other frequencies.

The acoustic emission time signature of a typical longitudinal matrix splitting failure is given in Fig. 6. This emission had an amplitude on the tape recorder of 1.7 volts (9.6 mv signal at the source, before

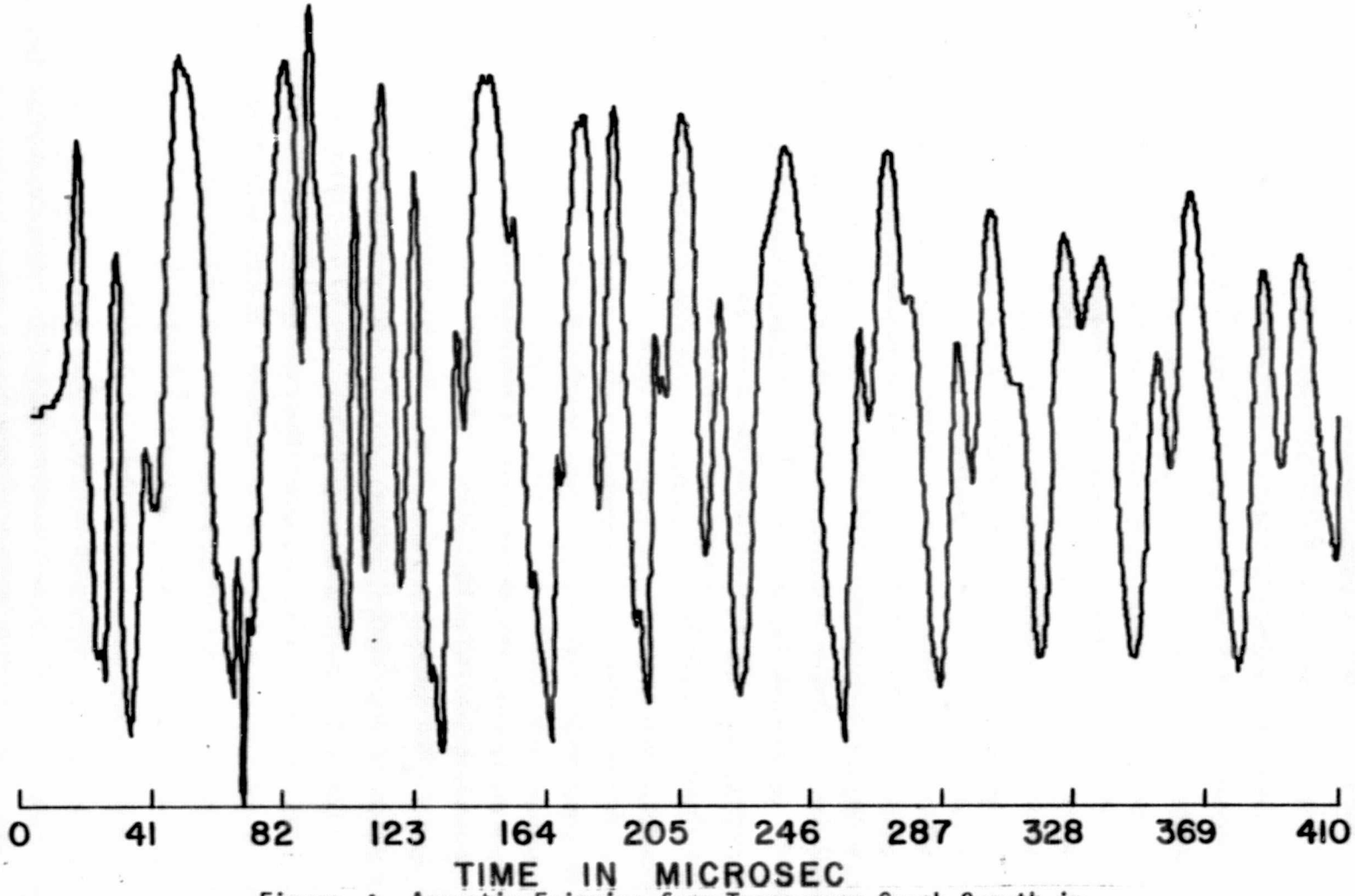

Figure 4. Acoustic Emission from Transverse Crack Growth in $[0_3]$ Specimen, Recorded by Transducer, Normalized with Respect to the Maximum Amplitude of 4.3 volts

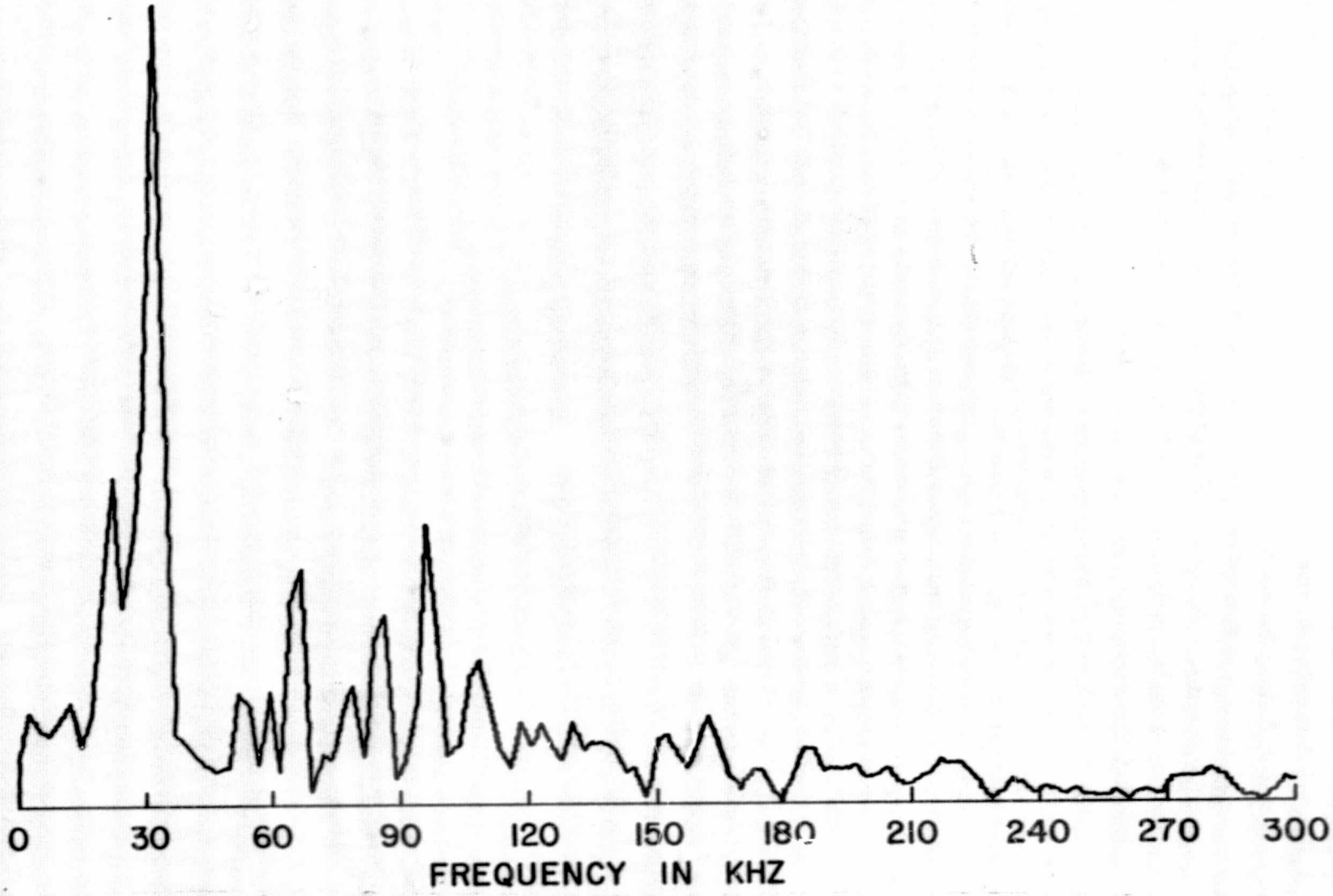

Figure 5. Fourier Transform of Acoustic Emission Shown in Figure 4, Recorded by Transducer from Transverse Crack Growth

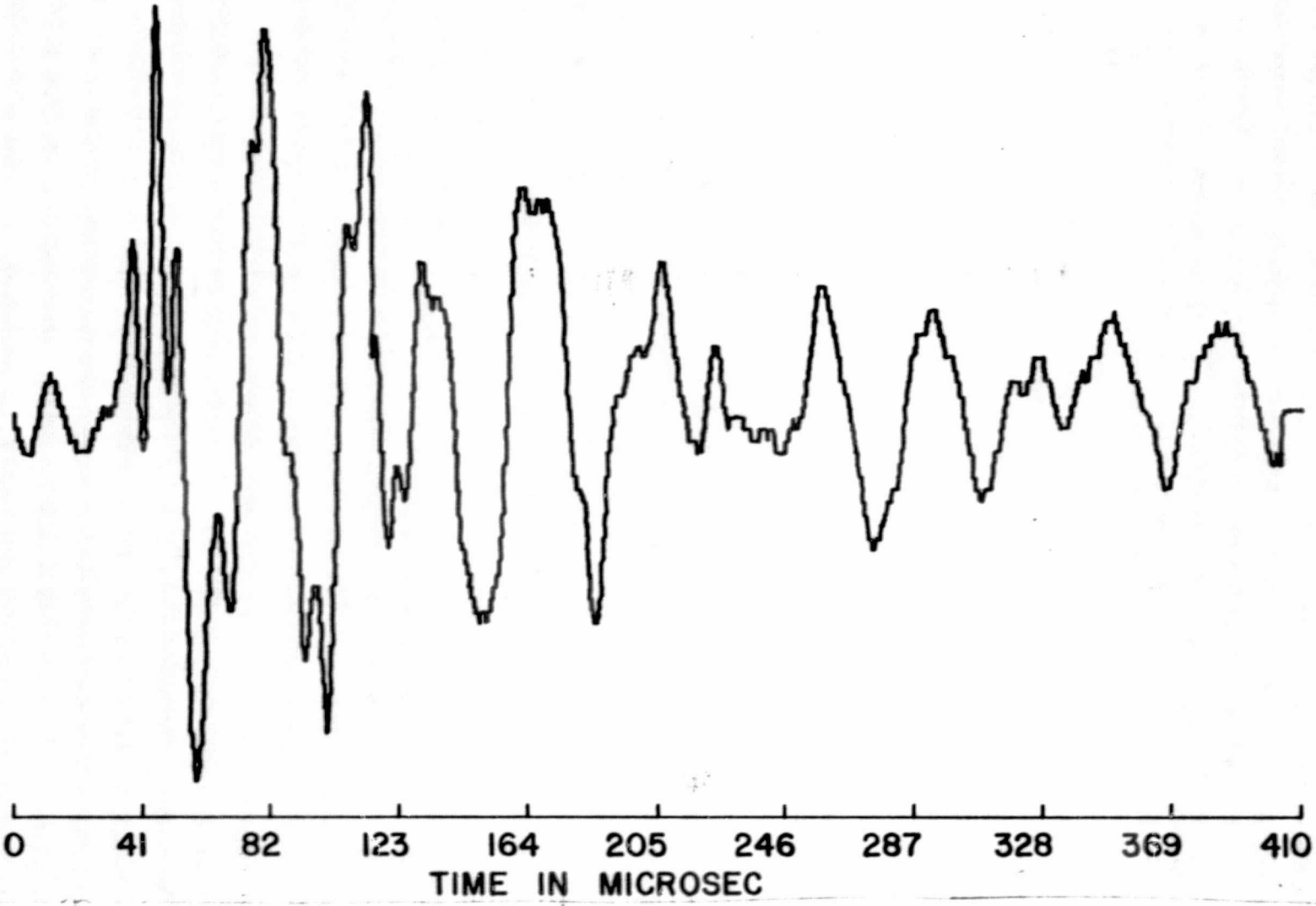

Fig. 6. Second Acoustic Emission from the Longitudinal Cracking of the [0_3] Specimen, Recorded by Transducer, Normalized with Respect to the Maximum Amplitude of 1.7 volts

amplification). The emission emanating from a longitudinal matrix splitting event has the following general characteristics. The time signature rises to a maximum amplitude very early in time, usually the first cycle, and decays rapidly. The frequency transform of this emission is shown in Fig. 7. Upon comparison of Fig. 7 and Fig. 5, one might note that the frequency spectrum of a matrix splitting event generally has broader frequency peaks while that for the transverse (fiber breakage) notch extension has a larger number of sharply defined peaks. This statement is, at the present time, simply a qualitative one. It is presently difficult to assign a quantitative parameter to describe this characteristic.

Additional time signatures for both longitudinal matrix splitting and fiber breakage events were given in reference 4. In summarizing those results the following was noted. The most notable feature of acoustic emissions from fiber breaks is the relatively large amplitude. Acoustic emissions from fiber breaks are usually twice as loud as acoustic emissions from matrix cracking in the specimens tested in this study. The emissions from fiber break failures start at less than the maximum amplitude of the emission. Usually 40 to 100 μsec. after the start of the emission the largest peak occurs. The amplitude declines only slightly in a 400 μsec time frame. A possible explanation for this behavior is that the crack moves intermittently across the fibers. That is, as the crack runs into new, unbroken fibers, it is momentarily halted until the stress in the fibers is increased to a level sufficient to break them. The crack will extend for some finite distance at a relatively slow rate in this fashion and finally halt. The energy of the event is thus added to the emission over some finite time period.

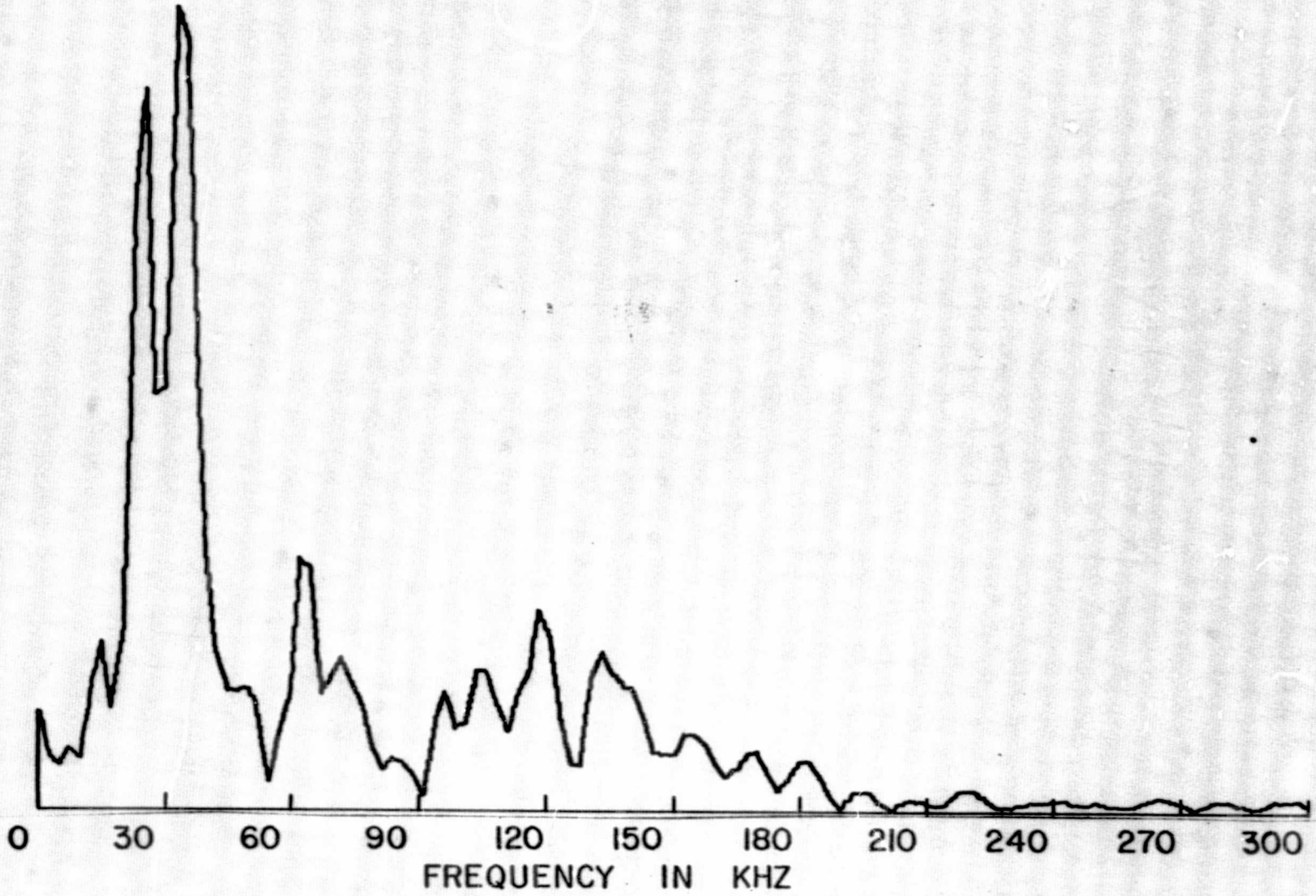

Figure 7. Fourier Transform of Acoustic Emission Shown in Figure 6, Recorded by Transducer from Longitudinal Crack Growth

But for certain exceptions, acoustic emissions from matrix cracking failure events are usually relatively low in amplitude. For the exceptions the crack ran rapidly for an unusually long distance. The typical emission from a matrix crack appears to be a single impulse that decays rapidly. These emissions start by rising to their maximum amplitude almost immediately relative to a 400 μsec. time frame, and usually within the first complete cycle. The emission usually has decayed to the background noise level before the end of the 400 μsec. time frame. Here it appears as if the matrix splitting crack runs its course at a rate very close to the wave speed in the material. The energy associated with the event is therefore released immediately causing the immediate rise in the AE time signal.

3. WORK PERFORMED SINCE LAST REPORTING PERIOD

3.1 Experimental Method

Since the last reporting period, the Department of Engineering Science and Mechanics has obtained a real-time digital spectrum analyzer based upon the Fast Fourier Transform (FFT) algorithm. This instrument, a DMS 5000 FFT Analyzer, Zonic Technical Laboratories, Inc., has been utilized to obtain time signatures and associated Fourier spectra of the acoustic emission signals that had been previously recorded on the data tape. This instrument significantly increases our capability of obtaining Fourier spectra of acoustic emission signals in terms of time and effort spent. Instead of the data analysis system shown schematically in Fig. 2, which required typically a total time of one day to obtain an amplitude-frequency plot from the coumputer center, the FFT Analyzer presents a completed plot in something less than 30 seconds. Hence the number of acoustic emission signals that can be analyzed is greatly increased.

In the results that follow, the acoustic emission events that had been recorded during the application of load to the $[0_3]$ specimens discussed in the previous chapter were utilized as input signals. Because the maximum frequency input to the Zonic FFT Analyzer is 100 KHz, it was necessary to first input the AE signal into the transient waveform recorder described in the previous chapter. This instrument digitizes and stores the transient signal and plays it back repetitiously in analog form at a fixed rate. As used in this case, the waveform recorder was set to store a signal having a time record length of 409.6 μsec and to play it back at a rate 25 times slower, thus playing back a time record of length 10.24 msec. In effect then a signal containing frequencies up to 300 KHz on the tape recorder is slowed down by the

transient recorder to represent a signal containing frequencies up to 12 KHz. This particular setting was chosen for the following reason. When a transient pulse (an AE event) is applied to a specimen, the energy in the pulse is transferred from those frequencies composing the pulse to the natural resonant frequencies of the specimen. This phenomenon is easily discernible on the time record of an AE event. Since it is desirable to obtain as much frequency information on the original AE pulse as possible, it is desirable to keep the time record used for analysis as short as possible. The time settings used above were the minimum available on our equipment.

The expanded analog signal from the transient waveform recorder was input to the Zonic with the latter adjusted to record the exact signal length of this waveform, i.e., 10.24 msec. For the Zonic Analyzer, this range corresponds to a maximum possible input frequency of 50 KHz. Since the expanded waveform represents a filtered signal having frequencies only up to 12 KHz, the frequency spectra presented in the next section must be interpreted as being meaningful only up to 12 KHz. The horizontal axis is set by internal software in the Zonic FFT and cannot be adjusted to expand the horizontal scale, which naturally would have been preferable. In each case, the time signal was plotted as received by the Zonic Analyzer, a half-hanning window was used to window the time signal, and the frequency spectrum of the windowed time signature was determined. The half-hanning window has the effect of emphasizing the initial portion of the transient signal and de-emphasizing the trailing portion. Thus the frequency components in the initial portion should be accentuated.

3.2 Results and Discussion

A large number of acoustic emission events from the $[0_3]$ specimens discussed in Sec. 2.1 were analyzed according to the procedure discussed in Sec. 3.1. The results of this analysis chosen for inclusion in this section are considered to be typical. In particular, the runs shown here were chosen because they corresponded to AE events which were more closely correlated to visual observations of the fiber breakage and longitudinal cracking failure modes.

The major difficulty with obtaining so much data, especially in the form obtained by signature analysis of a large number of different events, is that it becomes increasingly hard for the mind to sort out and identify distinguishing characteristics. In any even, the results appear to bear out for the most part the previous observations reported in Section 2.2. In particular the majority of AE events identified with either fiber breakage or matrix cracking have the general character identified in Sec. 2.2. There are, however, variations from this norm that cannot be completely accounted for at present. Whether these variations are due to signals from an event that was occurring outside the region observed under the microscope or whether they indicate that a particular failure mode does not always have the characteristic pattern is a question that cannot presently be answered.

Figure 8 is a time signature of an acoustic emission corresponding to fiber breakage as the previously described notch moved transversely to the applied load. This plot is a direct readout from the FFT analyzer. As such, the scale values are controlled by the software of the instrument. Thus because of the time expansion of the signal affected by the transient

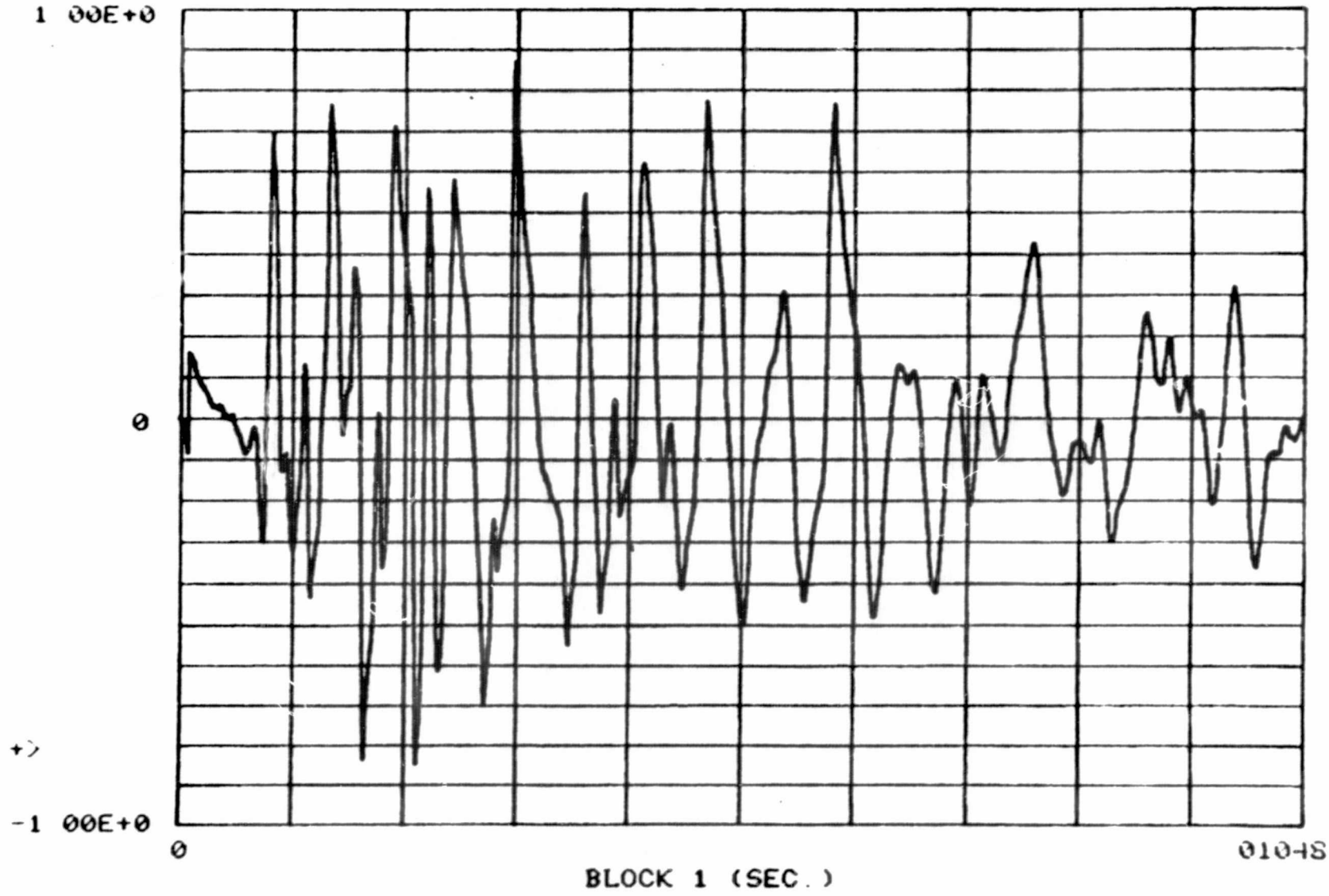

Figure 8. Acoustic Emission from Fiber Breakage Failure Event in [0_3] Specimen. Horizontal Scale Should Be Divided by 25 for Real Time Value.

recorder (as described in the preceding section) the horizontal time scale should in fact read 409.6 μsec full scale, that is, 25 times less than the value shown. (Note also that this scale is set digitally and should correspond to a power of two. An error in the software causes .01048 sec. to be printed out on the plot when in actuality the value should be .01024 sec). Figure 9 is the corresponding Fourier spectrum of this signal. The horizontal scale should be read here as 25 times that actually printed. Again, as discussed previously, frequency values larger than 12 KHz as shown on this plot are somewhat meaningless since these frequency components have been greatly reduced by filtering in the instrumentation. At the top of the graph, the phase angle is plotted versus frequency. The Fourier transform is initially calculated as a complex number. When the magnitude of this number is computed for display the phase angle is also calculated and displayed by the FFT system. Figure 10 is a plot showing a table of values for the sixteen largest frequency components present and their respective amplitudes, F1(N), and phase angles, F2(N).

A half-hanning window was applied to the time signal, Fig. 11, the Fourier spectrum was computed, Fig. 12, and the major frequency components plotted, Fig. 13. As seen in Fig. 11, the half-hanning window serves to reduce the trailing edge of the time signal to essentially zero, thus emphasizing the initial portion. The frequency spectrum, Fig. 12 then shows fewer low frequency components than Fig. 9 for the unwindowed signal. This is indicative of the fact that the trailing portion of the AE event, Fig. 8, contains mostly low frequency components. These are most likely to be associated with the natural resonances of the specimen and are undesirable when attempting to characterize the AE event.

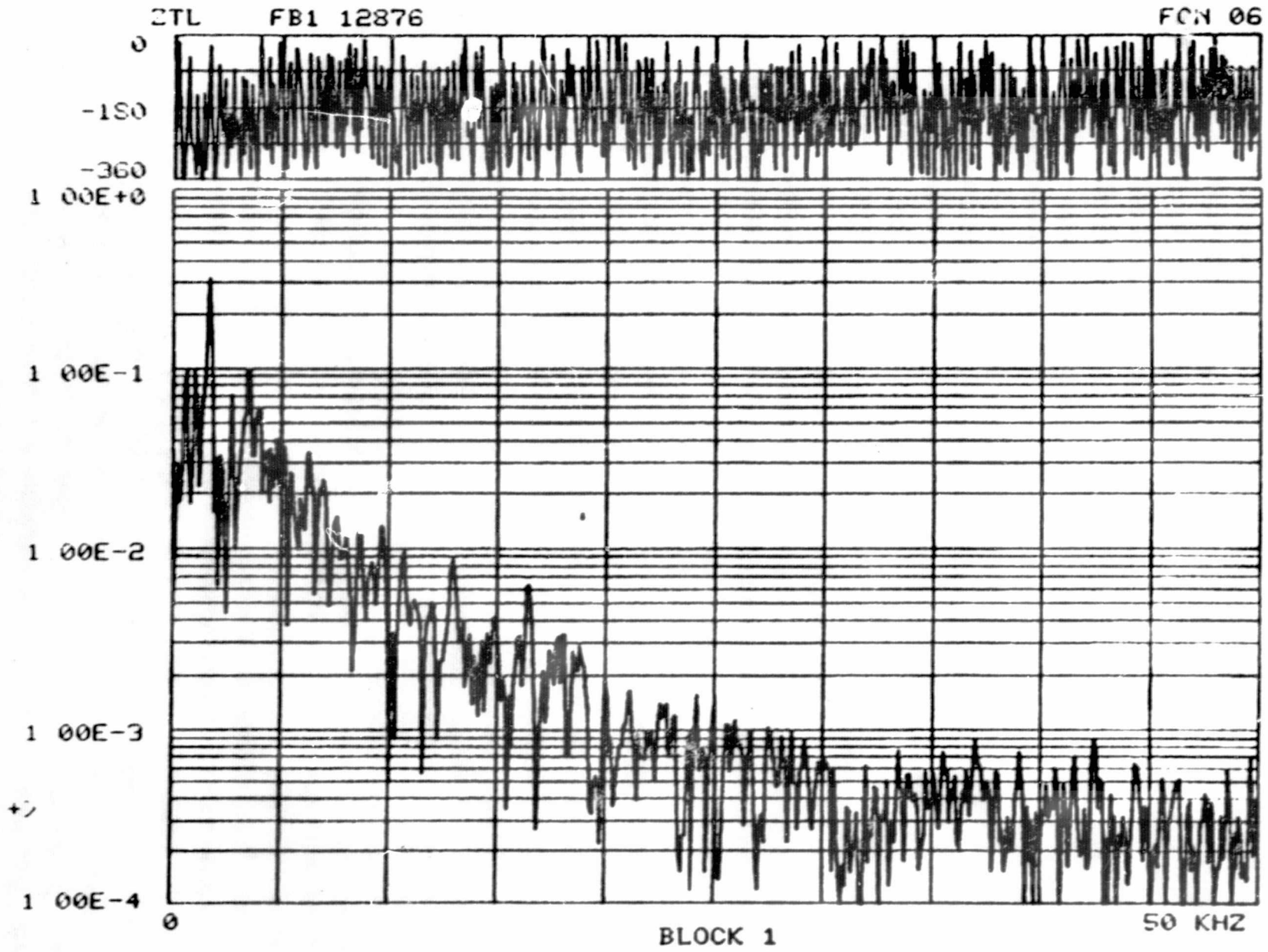

Figure 9. Fourier Transform of Acoustic Emission Event, Shown in Figure 8, from Fiber Breakage. Horizontal Scale Should Be Multiplied by 25 for True Frequency

```
+)   FB1 12876
+)
+)   ? 6
START FREQ    ? 10
END FREQ    ? 15000
SEARCH DISPLAY #? 1
# PEAKS? 16

RANK    CHANNEL NO.      FREQUENCY     F1(N)        F2(N)
1               18        1.75E+3     3.20E-1    -1.93E+2
2               11        1.07E+3     9.85E-2    -1.44E+2
3               36        3.51E+3     9.77E-2    -3.33E+2
4                7        6.82E+2     9.46E-2    -5.46E+1
5               28        2.73E+3     7.07E-2    -8.56E+1
6               41        4.00E+3     6.00E-2    -8.08E+0
7               50        4.88E+3     4.03E-2    -1.48E+1
8               53        5.17E+3     3.65E-2    -3.28E+2
9               47        4.58E+3     3.61E-2    -1.19E+2
10              45        4.39E+3     3.43E-2    -5.37E+1
11              65        6.34E+3     3.36E-2    -1.45E+2
12              23        2.24E+3     3.28E-2    -2.48E+2
13              21        2.05E+3     3.19E-2    -7.25E+1
14               3        2.92E+2     2.88E-2    -1.74E+2
15              56        5.46E+3     2.60E-2    -2.00E+2
16              72        7.03E+3     2.35E-2    -2.73E+2
+)
```

Figure 10. Plot of Frequencies Having Maximum Amplitudes in Fourier Transform Shown in Figure 9. Values Should Be Multiplied by 25 for True Frequency Values

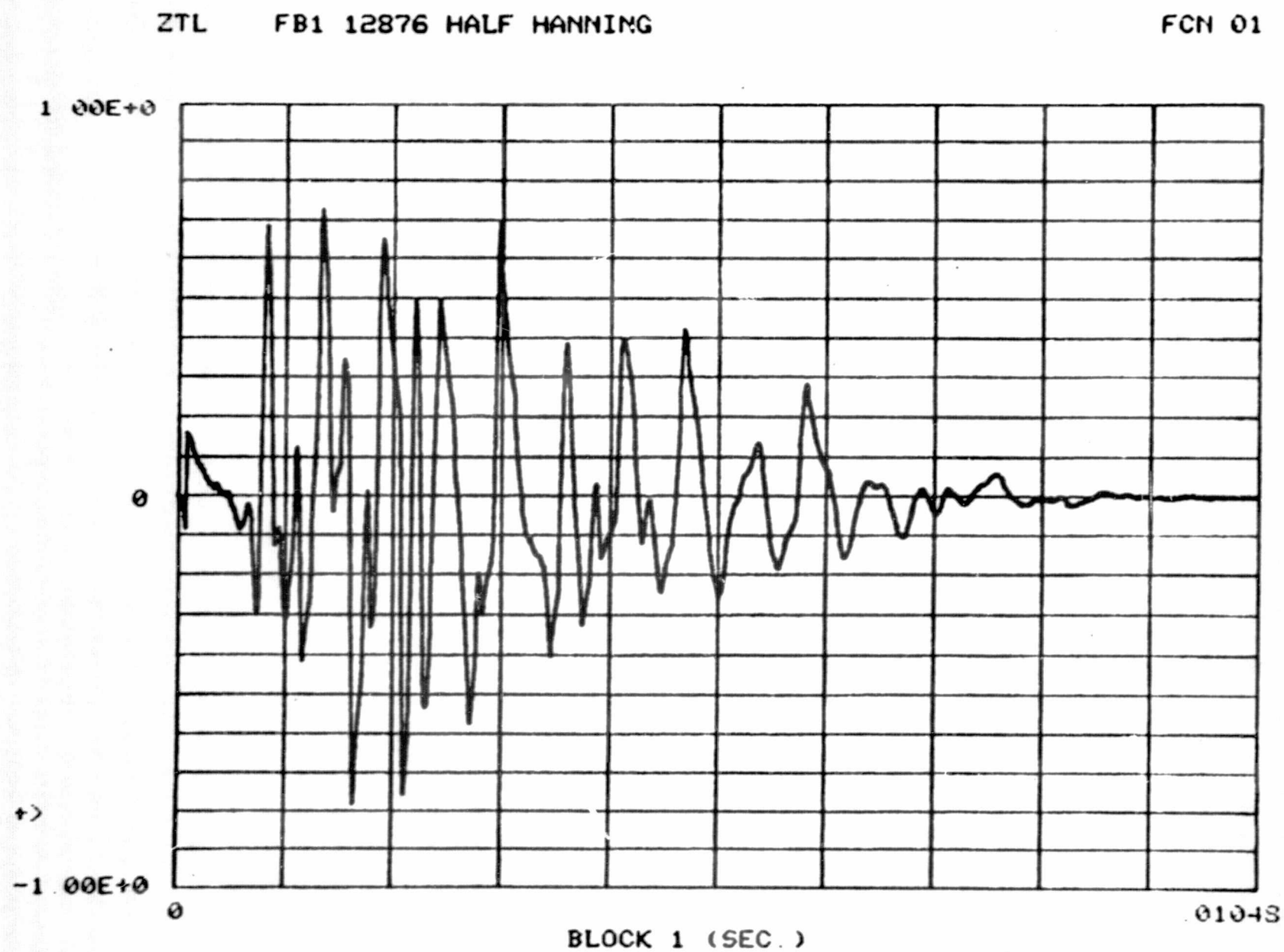

Figure 11. Acoustic Emission Event, Shown in Figure 8, from Fiber Breakage Failure after Windowing by Half-Hanning Window. Horizontal Scale Should Be Divided by 25 for Real Time Value

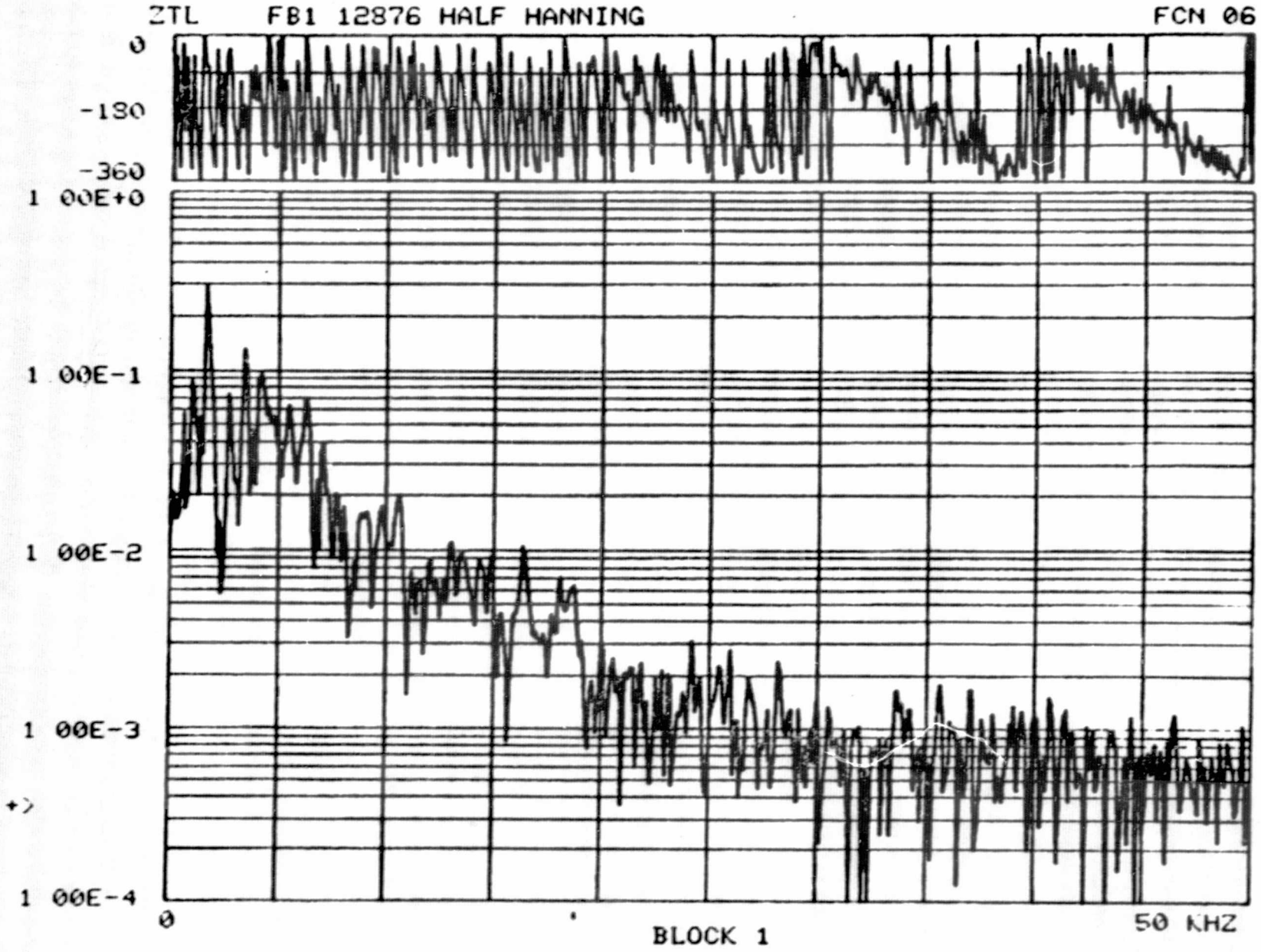

Figure 12. Fourier Transform of Windowed Time Signal Shown in Figure 11. Acoustic Emission from Fiber Breakage Failure Event. Horizontal Scale Should Be Multiplied by 25 for True Frequency Value

```
*   FFT 12STG HALF HANNING
*
*   ? 6
START FREQ    ? 10
END FREQ    ? 15000
SEARCH DISPLAY #? 1
# PEAKS? 16
```

RANK	CHANNEL NO.	FREQUENCY	F1(N)	F2(N)
1	18	1.75E+3	3.09E-1	-1.86E+2
2	36	3.51E+3	1.30E-1	-3.41E+2
3	44	4.29E+3	9.32E-2	-2.94E+2
4	11	1.07E+3	8.66E-2	-1.51E+2
5	28	2.73E+3	7.36E-2	-1.07E+2
6	65	6.34E+3	7.00E-2	-1.38E+2
7	57	5.56E+3	6.31E-2	-2.93E+2
8	47	4.58E+3	6.25E-2	-1.11E+2
9	7	6.82E+2	5.76E-2	-4.83E+1
10	50	4.88E+3	5.51E-2	-1.00E+1
11	15	1.46E+3	5.47E-2	-2.99E+0
12	40	3.90E+3	4.70E-2	-1.56E+2
13	73	7.12E+3	3.83E-2	-2.09E+1
14	70	6.83E+3	2.39E-2	-2.58E+2
15	2	1.95E+2	2.08E-2	-4.58E+1
16	79	7.71E+3	2.01E-2	-2.10E+2

*>

Figure 13. Plot of Frequencies Having Maximum Amplitudes in Fourier Transform Shown in Figure 12. Values Should Be Multiplied by 25 for True Frequency Values

Figure 14 shows the time signature of an acoustic emission event associated with longitudinal matrix splitting in the same $[0_3]$ specimen from which the fiber breakage AE event was taken for Fig. 8. Figures 15-17 display the windowed signal, the frequency spectrum after windowing and the table of largest frequency components present, respectively. The horizontal scales must again be interpreted as discussed above.

The fiber breakage event, Fig. 8, again is characterized by a time signature that continues to increase with time, reaching a maximum at approximately 120 μsecs (real time) after it started (3 msec on the scale of Fig. 8). The matrix signal, Fig. 14, attains its maximum amplitude by the second half-cycle. A new, interesting characteristic has been observed for these signals, as a direct result of plotting the data in the form of the FFT system. Comparison of Fig. 12 and Fig. 16 shows that the spectrum associated with a fiber breakage AE event usually has a larger number of individual, sharp peaks in the range 0-250 KHz than does the spectrum for the matrix splitting AE event. The peaks in the latter spectrum are much broader. On the other hand, if one visualizes an average curve plotted through the spectrum, i.e., an envelope of the curve, one can see that this "average curve" has a narrow peak and decays rapidly for the matrix splitting AE event while it is broader and flatter in the region 0-250 KHz for the fiber breakage event. In other words, the fiber breakage AE signal is more broad band than the matrix splitting AE signal.

Additional data on fiber breakage and matrix splitting AE events are included in Appendix A for informational purposes.

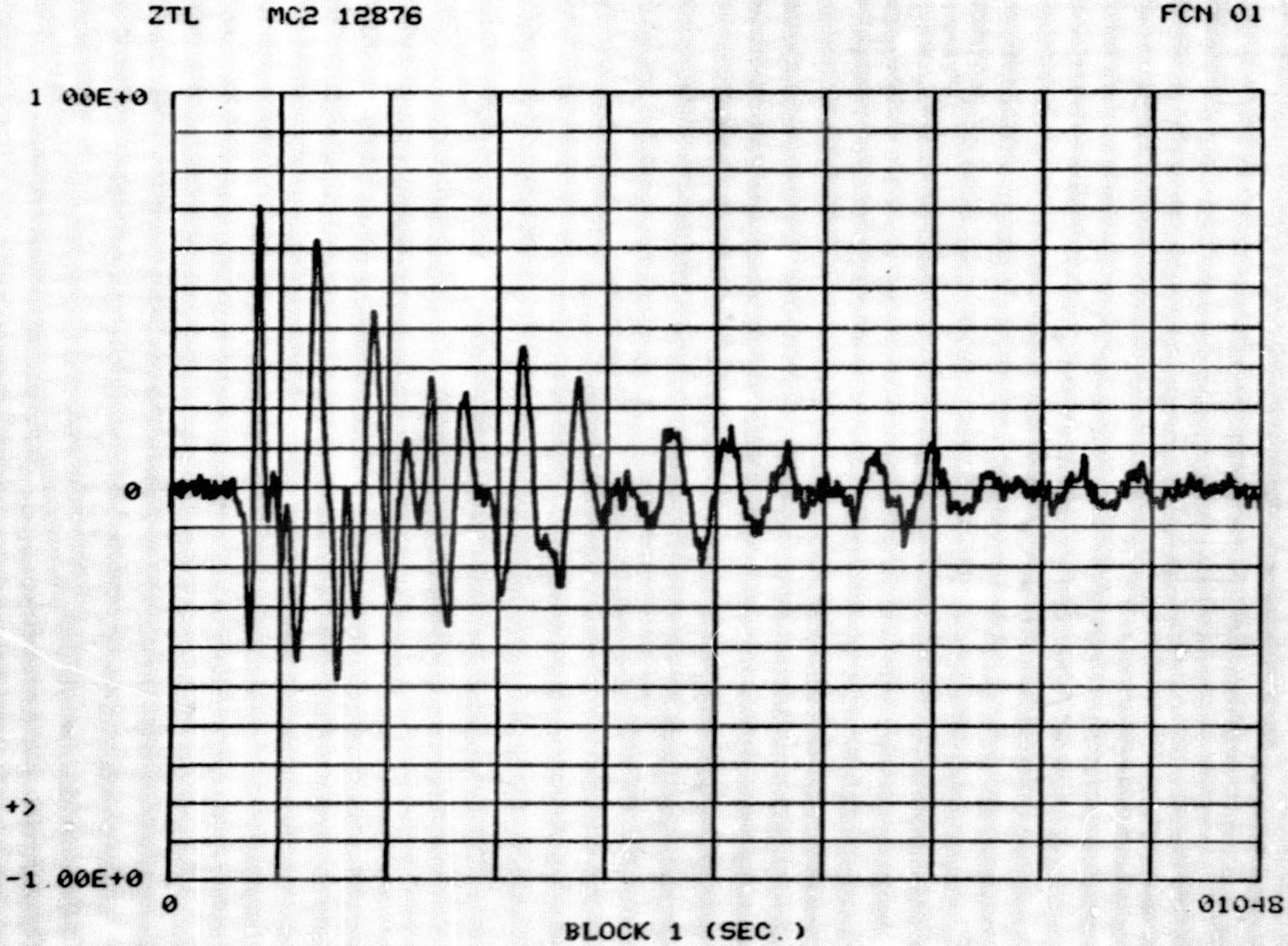

Figure 14. Acoustic Emission from Matrix Splitting Failure Event in $[0_3]$ Specimen.

Horizontal Scale Should Be Divided by 25 for Real Time Value

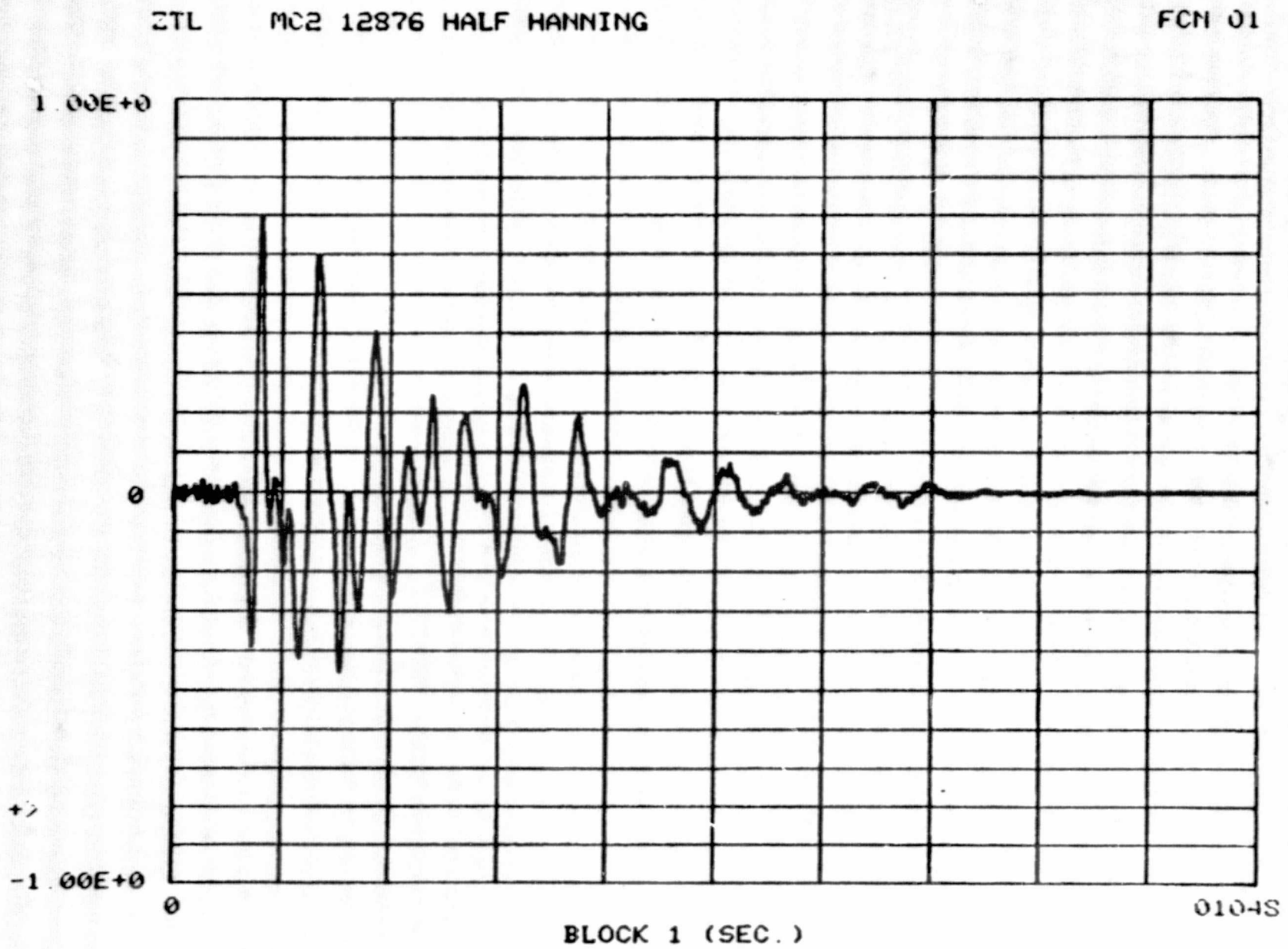

Figure 15. Acoustic Emission from Matrix Splitting Failure Event, Shown in Figure 14, after Windowing by Half-Hanning Window. Horizontal Scale Should Be Divided by 25 for Real Time Value

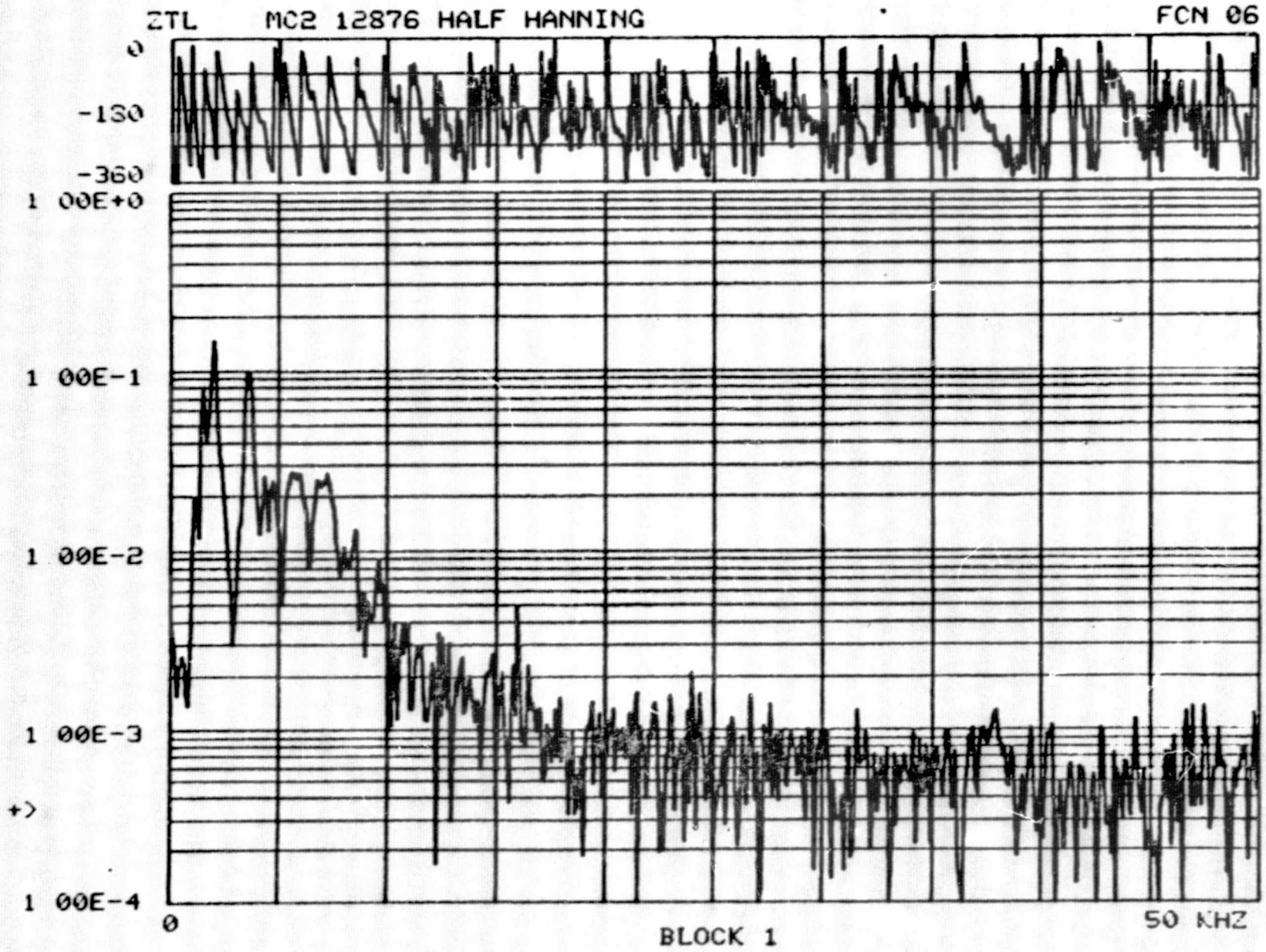

Figure 16. Fourier Transform of Windowed Time Signal from Matrix Splitting Failure Event, Shown in Figure 15. Horizontal Scale Should Be Multiplied by 25 for True Frequency Value

```
+   MC2 12S76 HALF HANNING
+>
+>   ? 6
START FREQ    ? 10
END FREQ    ? 15000
SEARCH DISPLAY #? 1
# PEAKS? 16

RANK    CHANNEL NO      FREQUENCY     F1(N)        F2(N)
1               21       2.05E+3     1.46E-1    -2.99E+2
2               37       3.61E+3     9.97E-2    -3.47E+2
3               16       1.56E+3     8.20E-2    -7.43E+1
4               58       5.66E+3     2.70E-2    -2.37E+2
5               62       6.05E+3     2.67E-2    -2.77E+1
6               75       7.32E+3     2.64E-2    -4.32E+1
7               45       4.39E+3     2.57E-2    -2.54E+2
8               70       6.83E+3     2.44E-2    -2.22E+2
9               49       4.78E+3     2.40E-2    -1.93E+1
10              12       1.17E+3     1.89E-2    -2.29E+2
11              88       8.59E+3     1.29E-2    -4.61E+1
12              83       8.10E+3     1.04E-2    -2.63E+2
13              99       9.66E+3     8.68E-3    -3.25E+2
14              85       8.30E+3     8.46E-3    -3.15E+2
15             101       9.86E+3     6.46E-3    -4.01E+1
16              92       8.98E+3     5.66E-3    -1.72E+2
+>
```

Figure 17. Plot of Frequencies Having Maximum Amplitudes in Fourier Transform Shown in Figure 16. Values Should Be Multiplied by 25 for True Frequency Values

4. SUMMARY AND CONCLUSIONS

The acoustic emission technique continues to hold promise for the study of failure mechanisms in composite materials. However, the present state-of-the-art is such that the technique leads to more frustration than to useful information. Studies that increase our understanding of the information contained in acoustic emission are making progress slowly and should be encouraged to continue. The present effort has found some interesting patterns in the acoustic emission time signatures that appear to characterize and distinguish matrix cracking from multiple fiber breakage. Difficulties encountered with the experiment preclude one's making a definitive statement concerning these patterns. The notched area in the tensile specimen was observed under a microscope while load was being applied. When a failure event was visually observed, a notation was made on the tape recording the data. Quite often, several acoustic emission events would occur on the tape at this location. While most of these AE events possess the pattern thought to be characteristic of the failure mechanism, quite often one or more of the AE signals had a different pattern. Because of the small observed area, it is impossible to say whether these different patterns were of significance to the observed failure or whether they resulted from failure events that occurred outside the field of view and therefore were not identified.

It does seem reasonable to suggest, based upon the preponderance of data, that separate failure mechanisms can be characterized by the acoustic emission time signatures for the graphite-epoxy specimens tested here. In particular, it was found that acoustic emission from fiber breakage events had time signatures that slowly increased to a

maximum amplitude and slowly decayed subsequently. Acoustic emission from matrix splitting failure, on the other hand, achieved a maximum amplitude by the second half-cycle and rapidly decayed subsequently. These patterns are distinctive enough that it is easy to identify one from the other.

Recent use in this program of an FFT analyzer and its associated data displays has led to the discovery of a possibly distinctive pattern in the Fourier spectra of the acoustic emission signals from the two different failure mechanisms studied. The spectrum of an AE signal from a fiber breakage event typically is composed of a large number of sharp frequency peaks in the range 0-300 KHz. The spectrum of an AE signal from a matrix cracking event has fewer frequency peaks and these are typically broader. Also, if one considers the envelope of the frequency spectra, the envelope for the fiber breakage signals is typically broader and flatter than that for the matrix splitting event. Thus it would appear that even though the majority of each frequency spectrum is composed of natural frequencies of the specimen, transducer and combined system, the different failure events excite the natural frequencies in a preferential fashion and therefore might be identified by appropriate pattern recognition schemes.

5. REFERENCES

1. "Signature Analysis of Acoustic Emissions from Composites," Semi-Annual Progress Report for the period October 1, 1975 - March 30, 1976, NASA Grant NSG 1238, Edmund G. Henneke, II and Carl T. Herakovich, April 1976.

2. "Signature Analysis of Acoustic Emissions from Composites," Semi-Annual Progress Report for the period April 1, 1976 - September 30, 1976, NASA Grant NSG 1238, Edmund G. Henneke, II, Carl T. Herakovich, and Samuel S. Russell, November, 1976.

3. "Signature Analysis of Acoustic Emissions from Composites," Semi-Annual Progress Report for the period October 1, 1976 - March 31, 1977, NASA Grant NSG 1238, Edmund G. Henneke,II, and Samuel S. Russell, April 1977.

4. "Signature Analysis of Acoustic Emissions from Composites," Interim Report for the period April 1, 1977 - September 30, 1977, NASA Grant NSG 1238, Samuel S. Russell and Edmund G. Henneke, II.

5. "Signature Analysis of Acoustic Emission from Graphite/Epoxy Composites," Thesis, Master of Science, Department of Engineering Science and Mechanics, Virginia Polytechnic Institute and State University, June 1977.

6. "A Microprocessor-Based System for Laboratory Data Acquisition," Master's Thesis, Virginia Polytechnic Institute and State University, 1975, G. H. Wilson, III.

APPENDIX A

Herein contained are a number of additional AE time signals and associated frequency spectra. These are added for informational purposes and in the desire for more completeness. Each plot was obtained from the DMS 5003 FFT analyzer and must be read with the same scaling factor changes discussed in the text. Thus, the time scale for each time signature should be divided by a factor of 25 so that the full scale value should read 409.6 μsecs. Similarly, each frequency plot has a frequency scale that should be read as 25 times that shown. Since the frequency bandwidth of the recorder was 300 KHz, only those frequencies between 0 - 12 KHz as shown on the plots are meaningful (corresponding to 0 - 300 KHz true frequency values).

The graphs are coded as follows: In the title at upper left, the letters FB denote an AE signal that was believed to arise from a fiber breakage event. The letters MC correspondingly denote a matrix crack failure. The numbers are test numbers. The letters HH are added to those signals that have been windowed by a half-hanning window. This window has the appearance of one-quarter of a cosine wave and hence serves to reduce the signal amplitude at the end of the time window.

ZTL MC4 12876 FCN 01

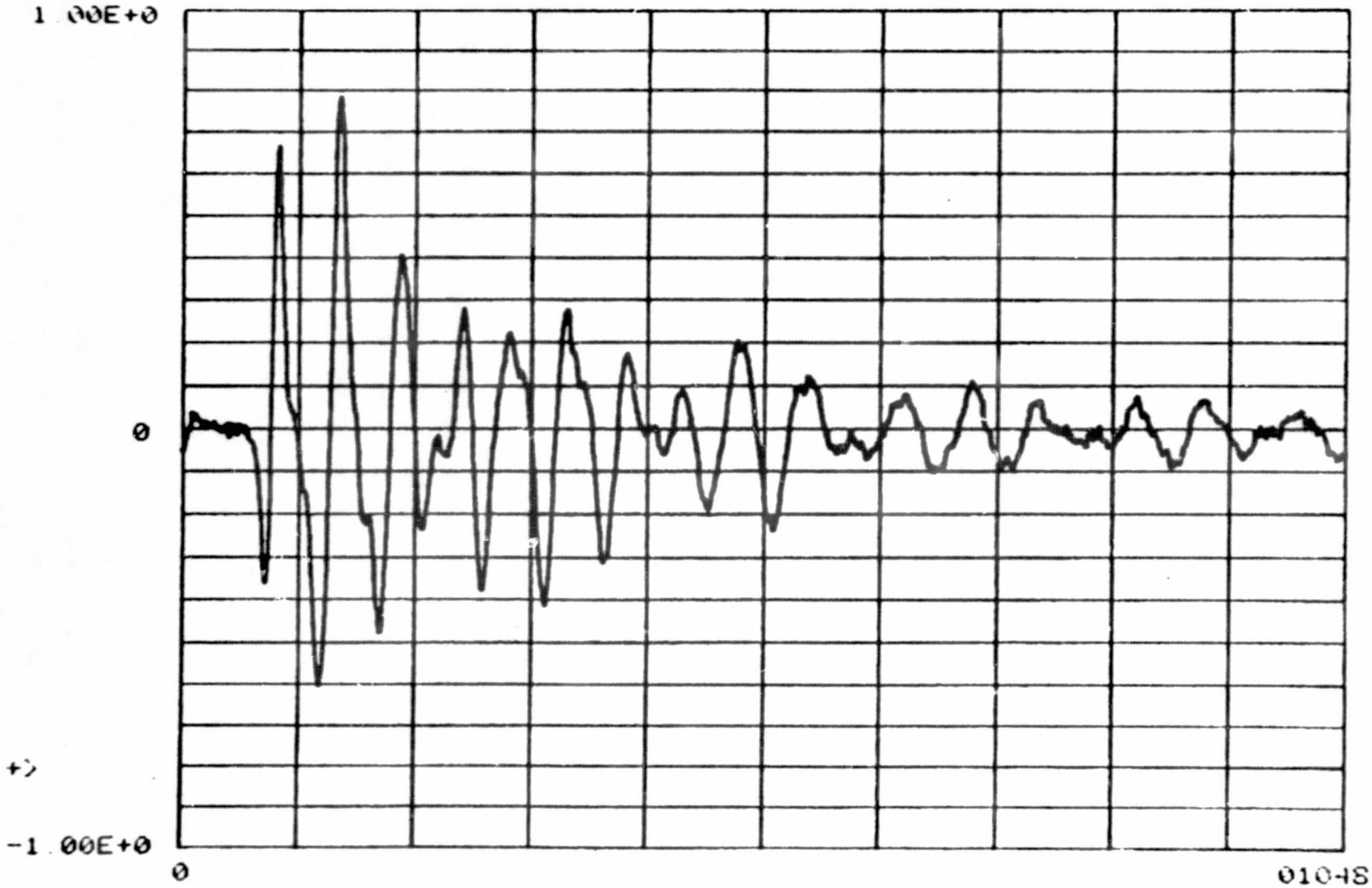

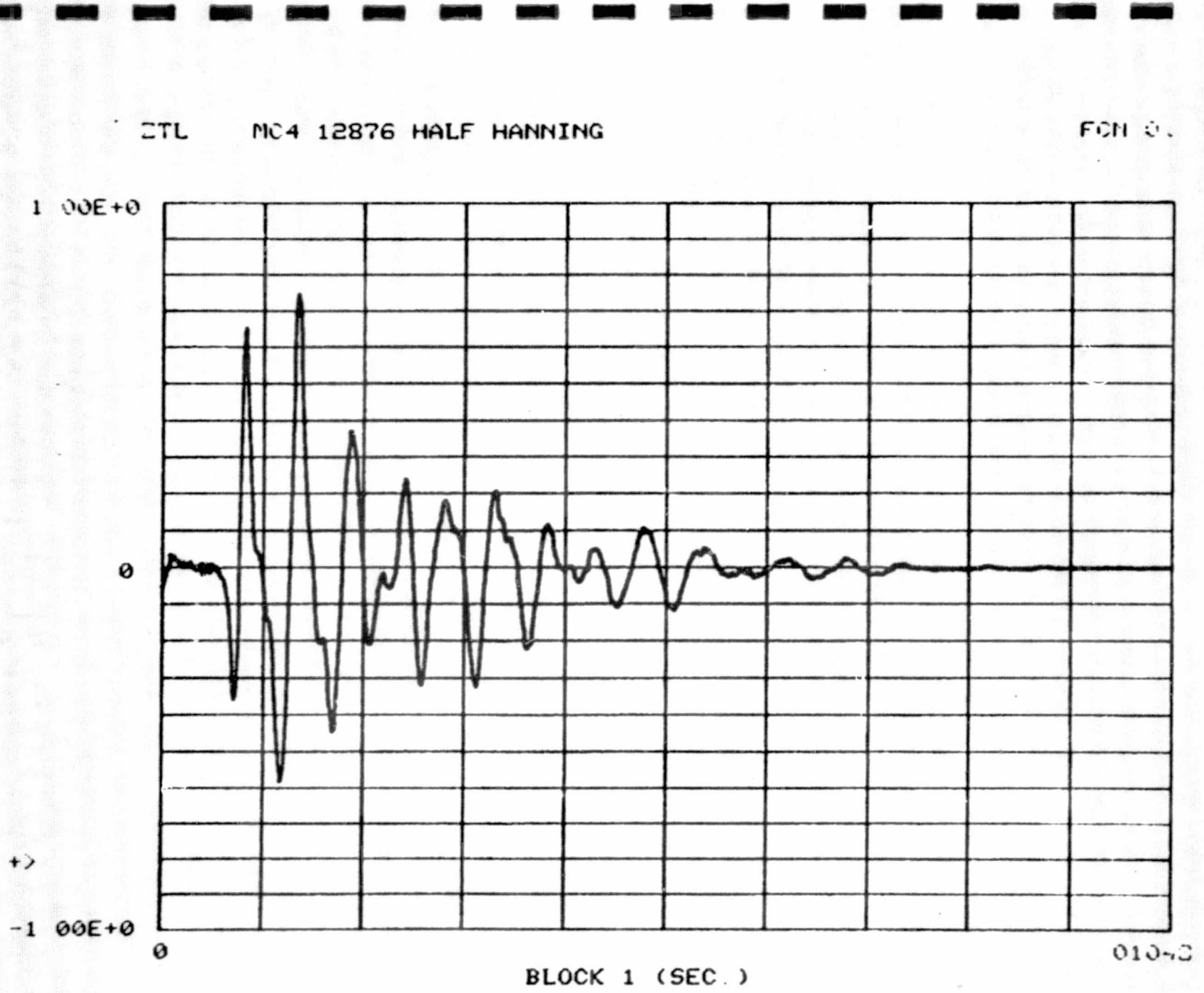
ZTL MC4 12876 HALF HANNING
FCN 0
1 00E+0
0
+>
-1 00E+0
0
010-3
BLOCK 1 (SEC.)

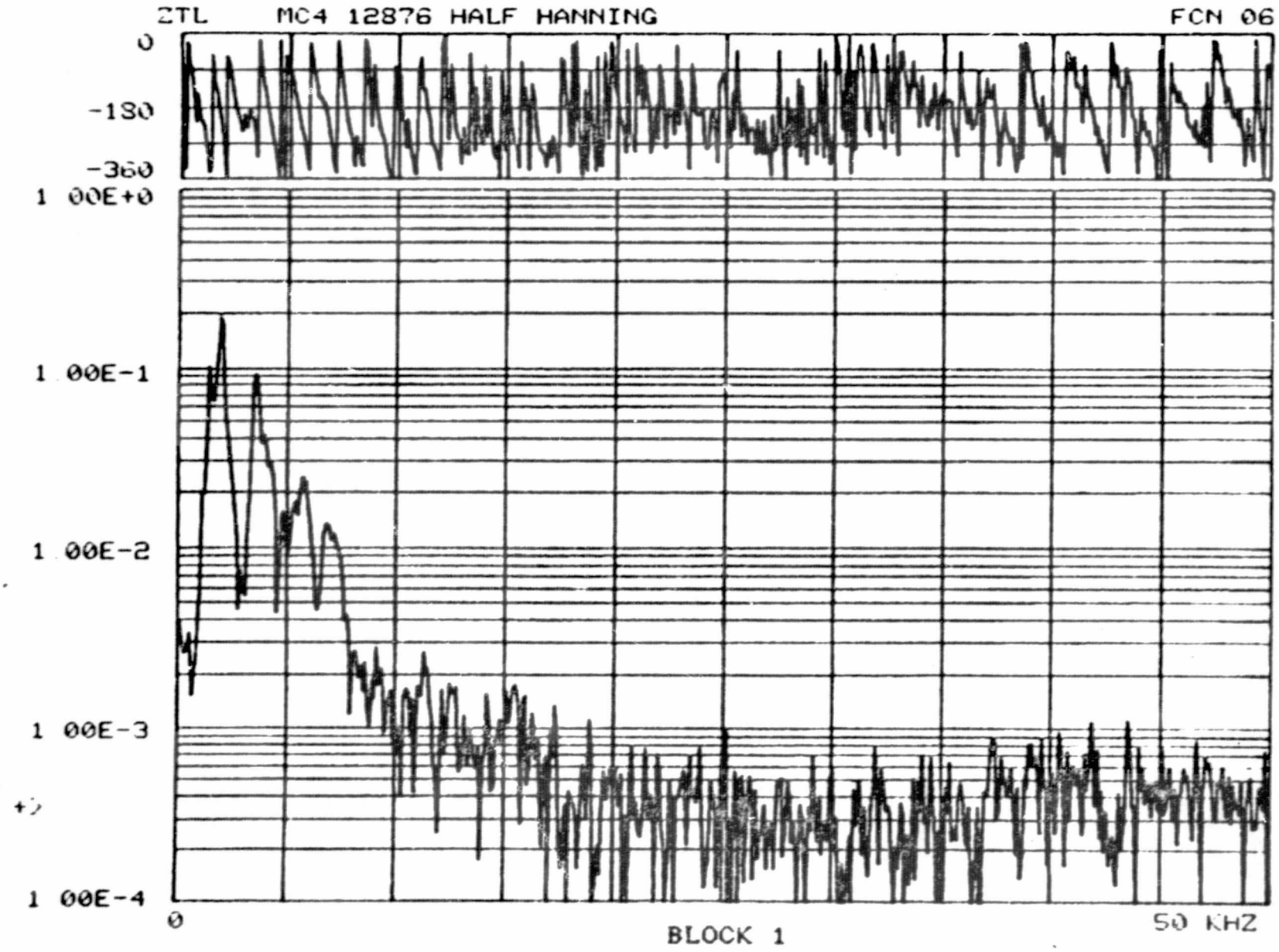
ZTL
MC4 12876 HALF HANNING
FCN 06
0
-180
-360
1 00E+0
1 00E-1
1 00E-2
1 00E-3
1 00E-4
0
50 KHZ
BLOCK 1

CTL FB1 12976 FCN 01

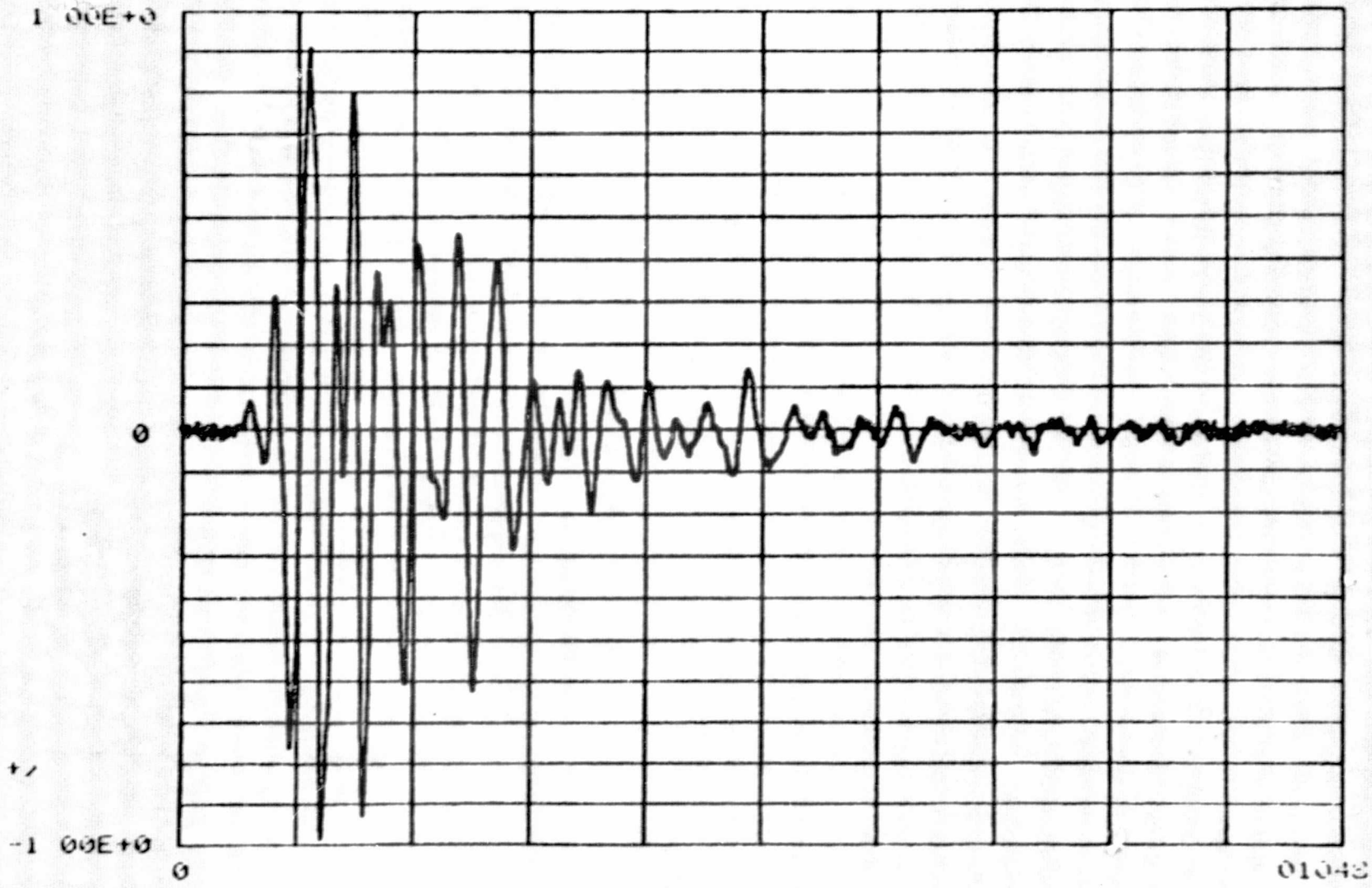

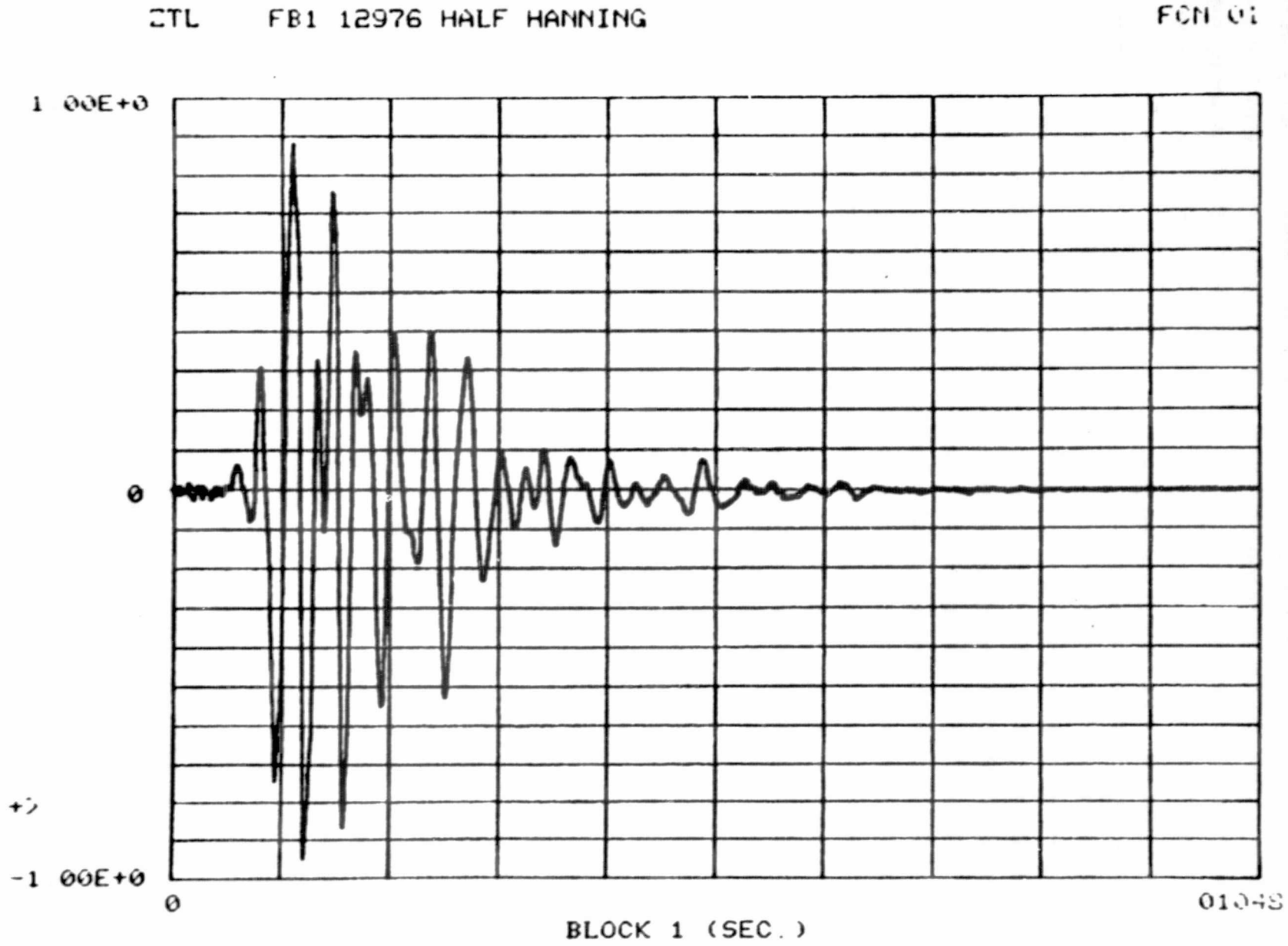
CTL FB1 12976 HALF HANNING
FCN 01
1.00E+0
0
+
-1.00E+0
0
01048
BLOCK 1 (SEC.)

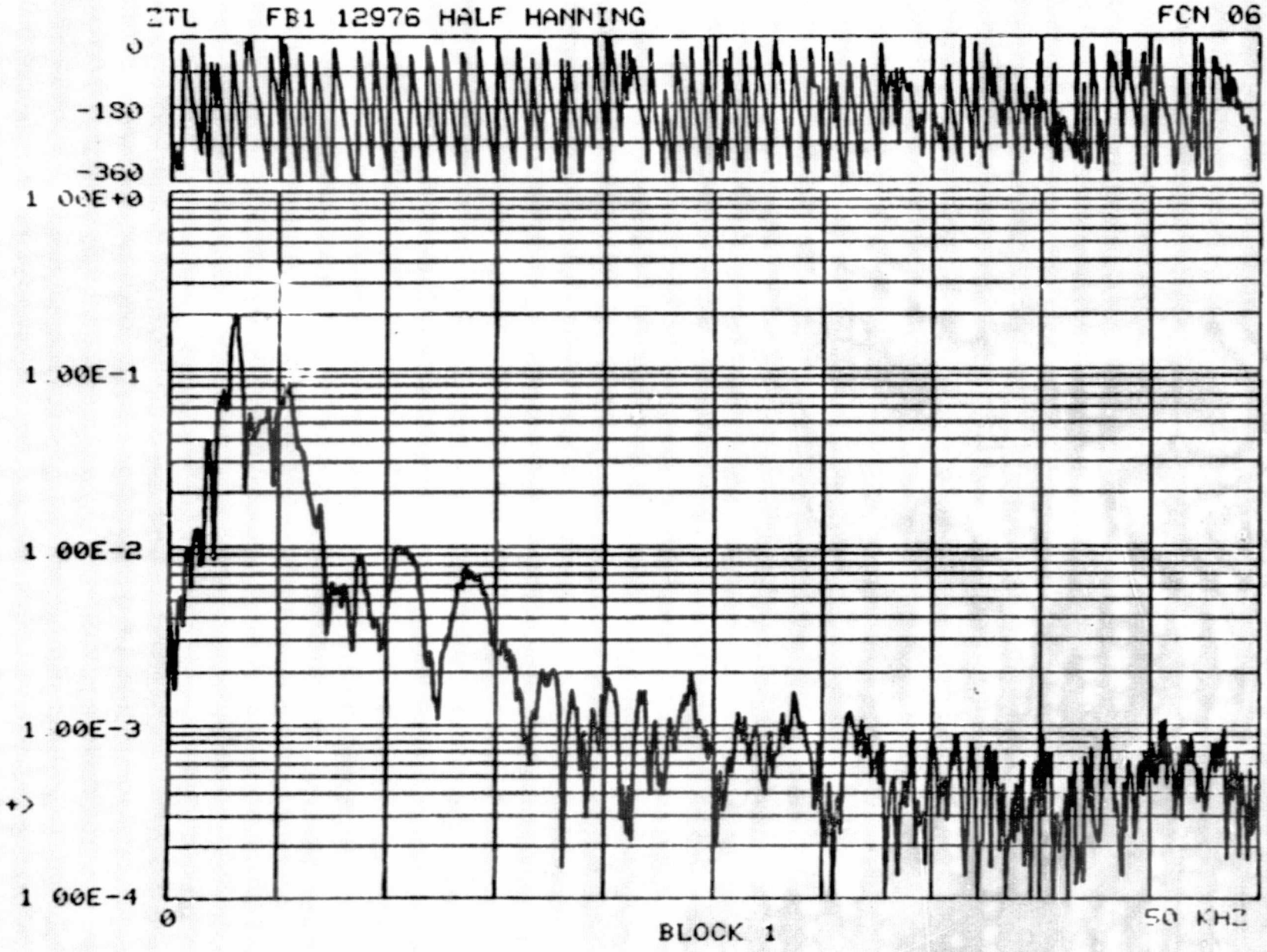
ZTL
FB1 12976 HALF HANNING
FCN 06
0
-180
-360
1.00E+0
1.00E-1
1.00E-2
1.00E-3
1.00E-4
+>
0
50 KHZ
BLOCK 1

```
+>   FB1 12976 HALF HANNING
+>
+>   ? 6
START FREQ    ? 10
END FREQ      ? 15000
SEARCH DISPLAY #? 1
# PEAKS? 16

RANK    CHANNEL NO.      FREQUENCY     F1(N)         F2(N)
1               31        3.02E+3     2.00E-1    -1.49E+2
2               56        5.46E+3     8.35E-2    -1.36E+2
3               26        2.53E+3     7.56E-2    -2.97E+2
4               24        2.34E+3     6.51E-2    -2.07E+2
5               47        4.58E+3     6.05E-2    -3.98E+1
6               38        3.71E+3     5.51E-2    -6.07E+1
7               43        4.19E+3     5.07E-2    -2.30E+2
8               19        1.85E+3     3.98E-2    -6.48E+1
9               62        6.05E+3     3.63E-2    -8.83E+1
10              71        6.93E+3     1.69E-2    -1.76E+2
11              13        1.26E+3     1.22E-2    -2.52E+2
12             108        1.05E+4     9.85E-3    -1.90E+2
13               9        8.78E+2     9.63E-3    -1.16E+2
14             112        1.09E+4     9.51E-3    -3.51E+2
15              91        8.88E+3     8.87E-3    -1.39E+2
16             115        1.12E+4     8.53E-3    -1.27E+2
+>
```

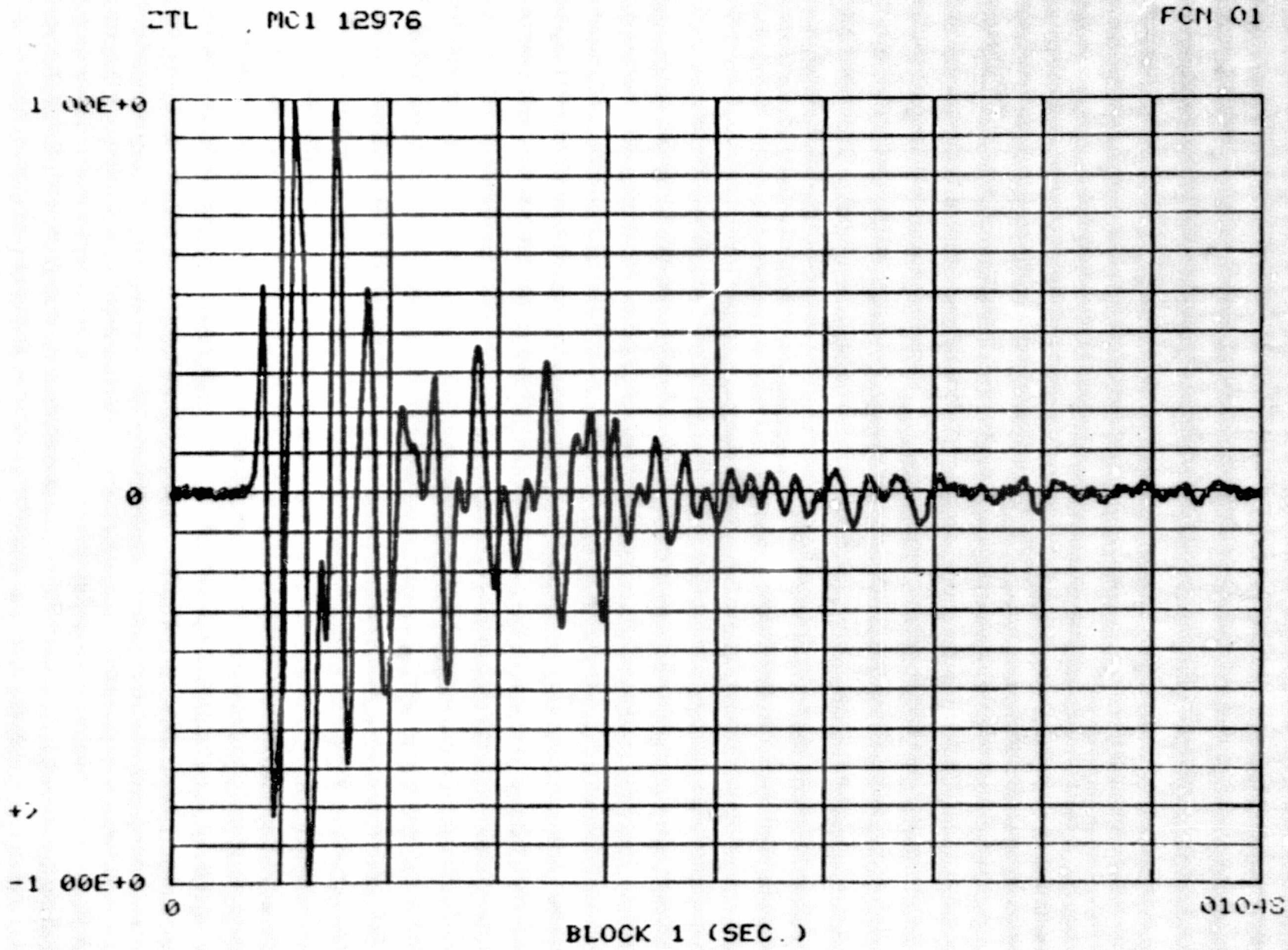
ZTL MC1 12976
FCN 01
1 00E+0
0
-1 00E+0
0
010-13
BLOCK 1 (SEC.)

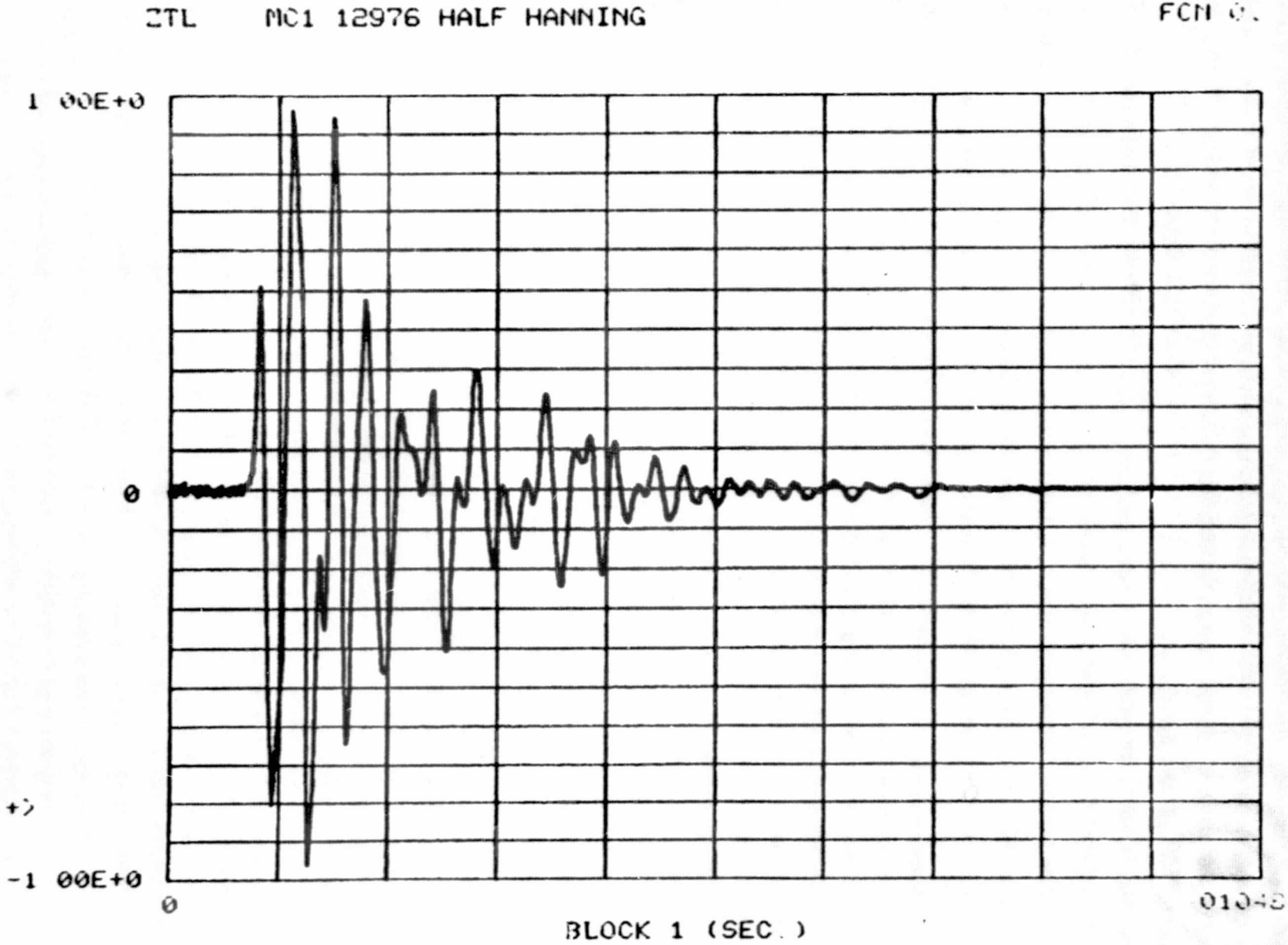
ZTL MC1 12976 HALF HANNING
FCN 0.
1.00E+0
0
+)
-1.00E+0
0
01048
BLOCK 1 (SEC.)

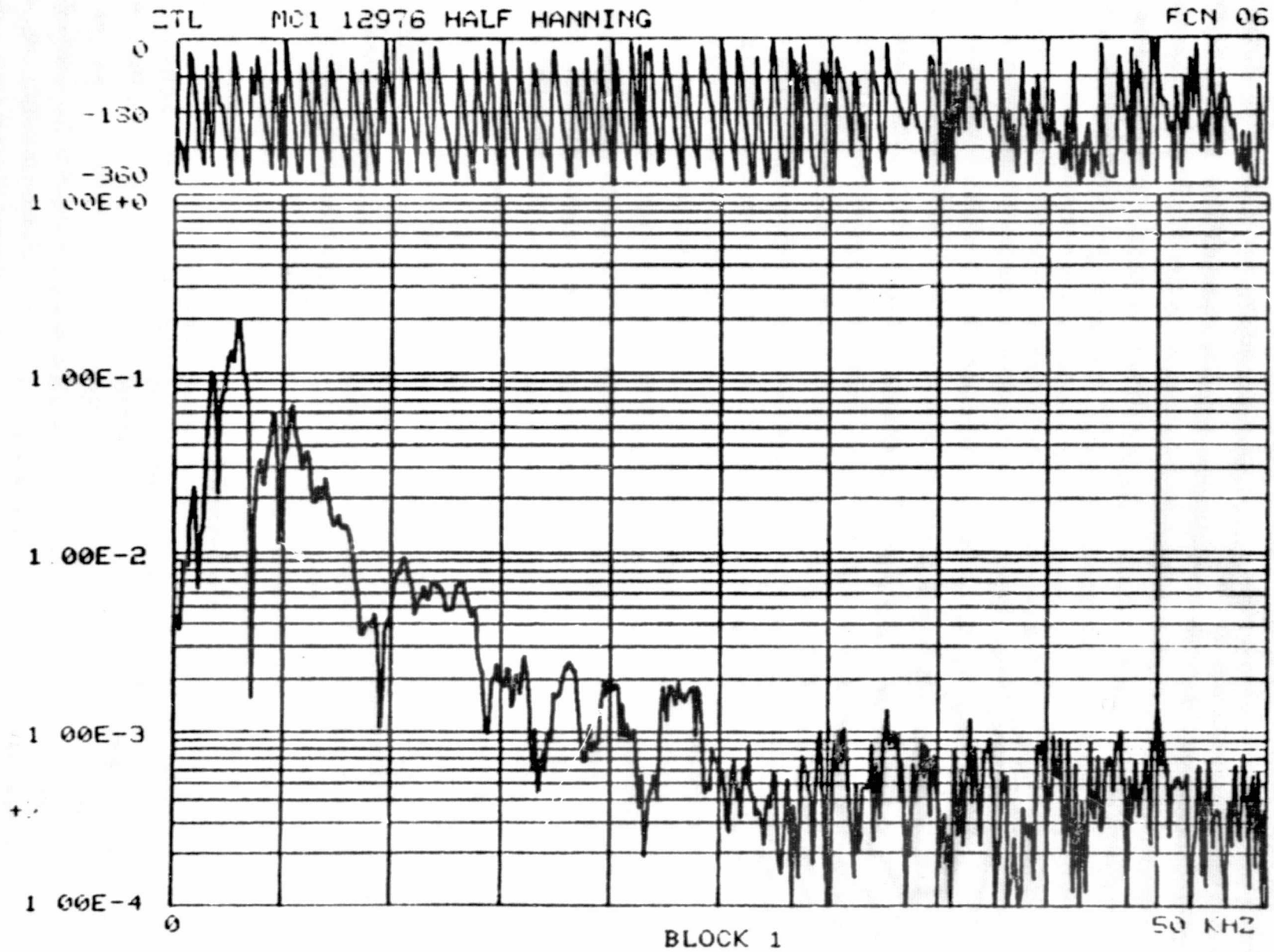
CTL MC1 12976 HALF HANNING
FCN 06
0
-180
-360
1.00E+0
1.00E-1
1.00E-2
1.00E-3
1.00E-4
0
50 KHZ
BLOCK 1

```
*   MC1 12976 HALF HANNING
*
*   ? 6
START FREQ    ? 10
END FREQ.   ? 15000
SEARCH DISPLAY #? 1
# PEAKS? 16

RANK    CHANNEL NO.      FREQUENCY     F1(N)        F2(N)
1               30        2.92E+3     1.94E-1    -1.50E+2
2               27        2.63E+3     1.32E-1    -2.79E+1
3               18        1.75E+3     1.00E-1    -2.24E+1
4               56        5.46E+3     6.56E-2    -2.31E+2
5               47        4.58E+3     6.00E-2    -9.60E+1
6               63        6.15E+3     3.67E-2    -1.90E+2
7               41        4.00E+3     3.28E-2    -1.75E+2
8               72        7.03E+3     2.54E-2    -3.54E+2
9               10        9.76E+2     2.30E-2    -1.91E+2
10              69        6.73E+3     2.30E-2    -2.16E+2
11              78        7.61E+3     1.58E-2    -2.14E+2
12              82        8.00E+3     1.41E-2    -3.56E+2
13             109        1.06E+4     9.28E-3    -8.38E+1
14               6        5.85E+2     8.78E-3    -2.87E+1
15             106        1.03E+4     7.97E-3    -3.14E+2
16             136        1.32E+4     6.87E-3    -1.96E+2
+>
```

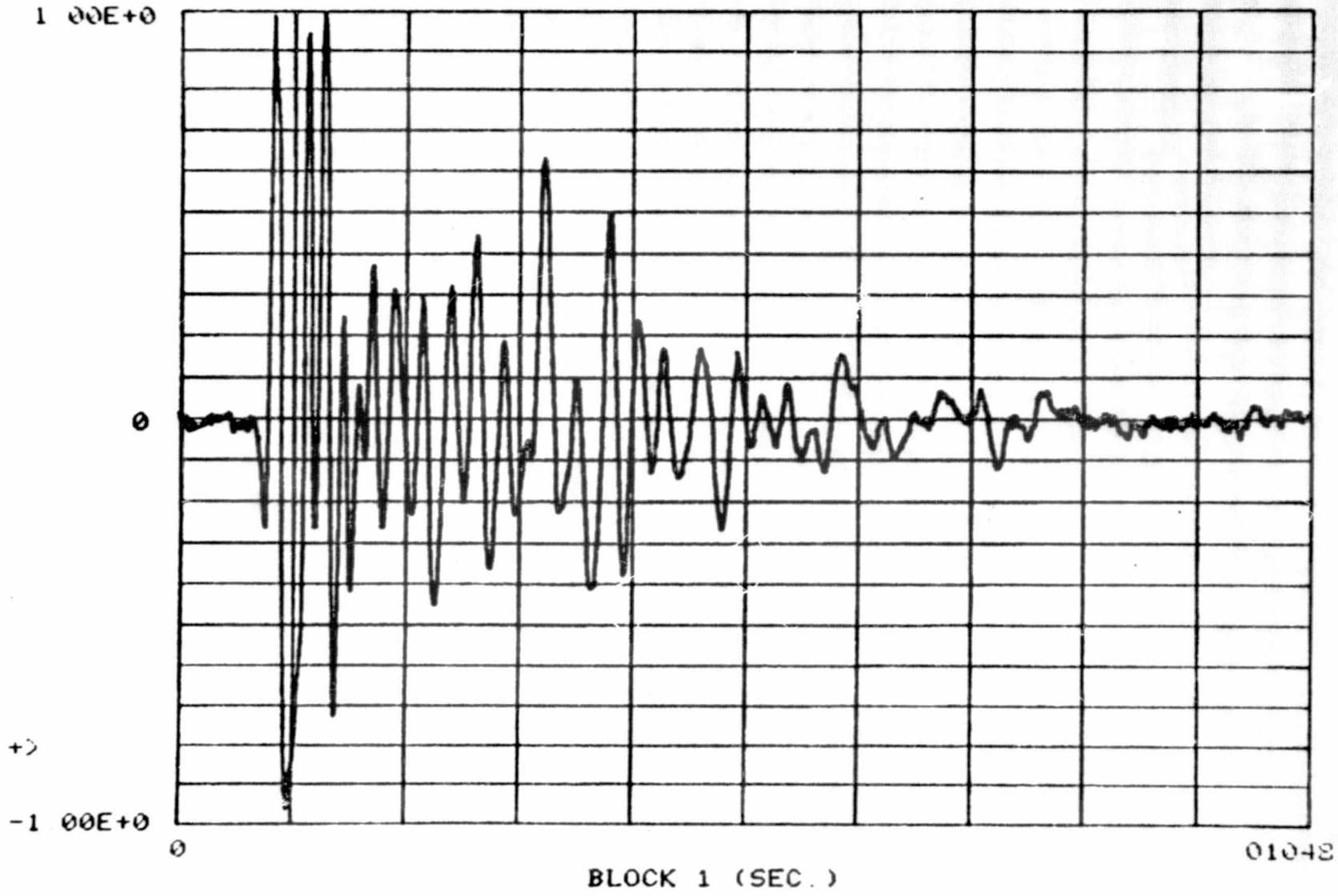
ZTL FB2 62377
FCN 01
1 00E+0
0
+)
-1 00E+0
0
01048
BLOCK 1 (SEC.)

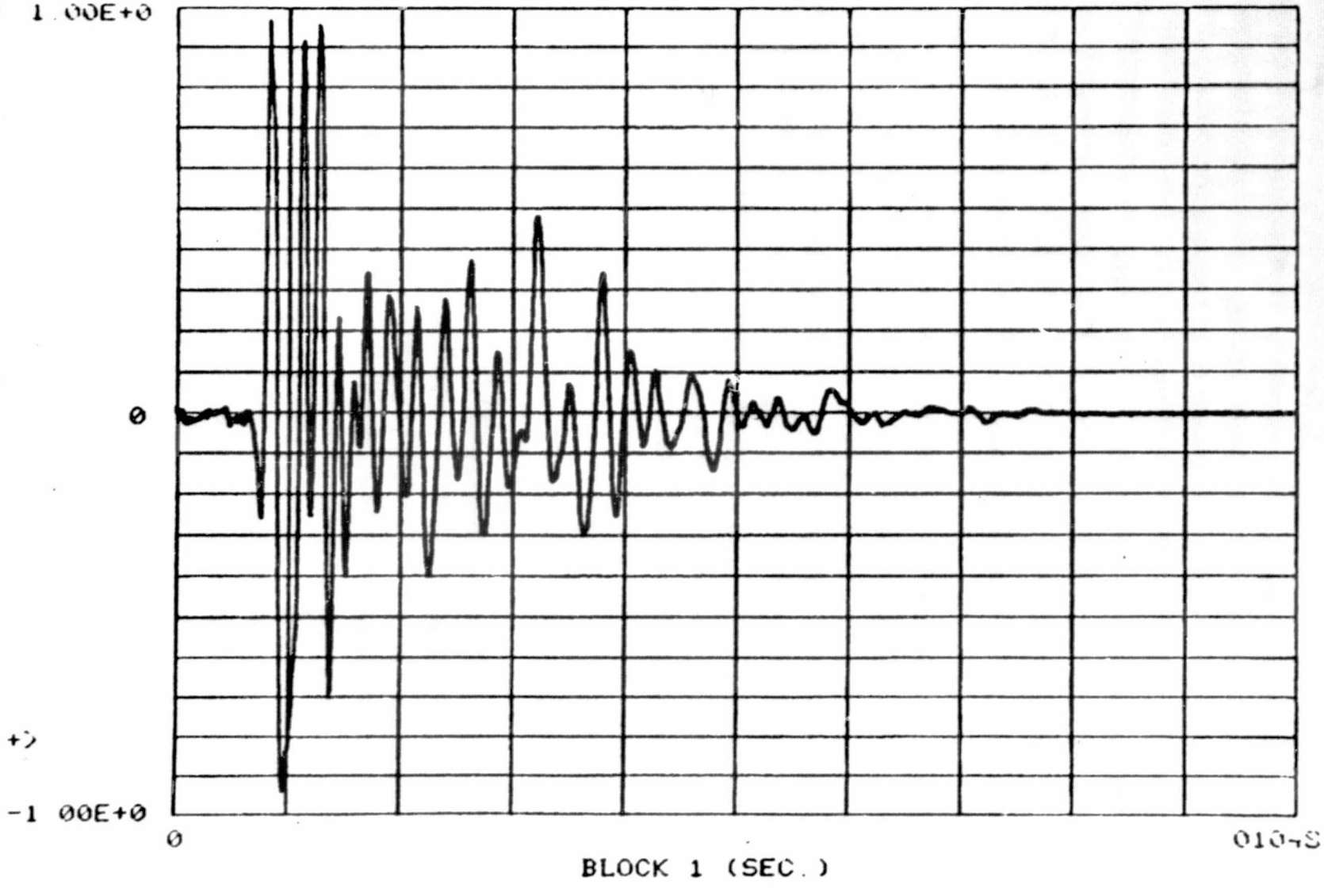
ZTL FB2 HH 62377
FCN 01
1.00E+0
0
+)
-1.00E+0
0
010-S
BLOCK 1 (SEC.)

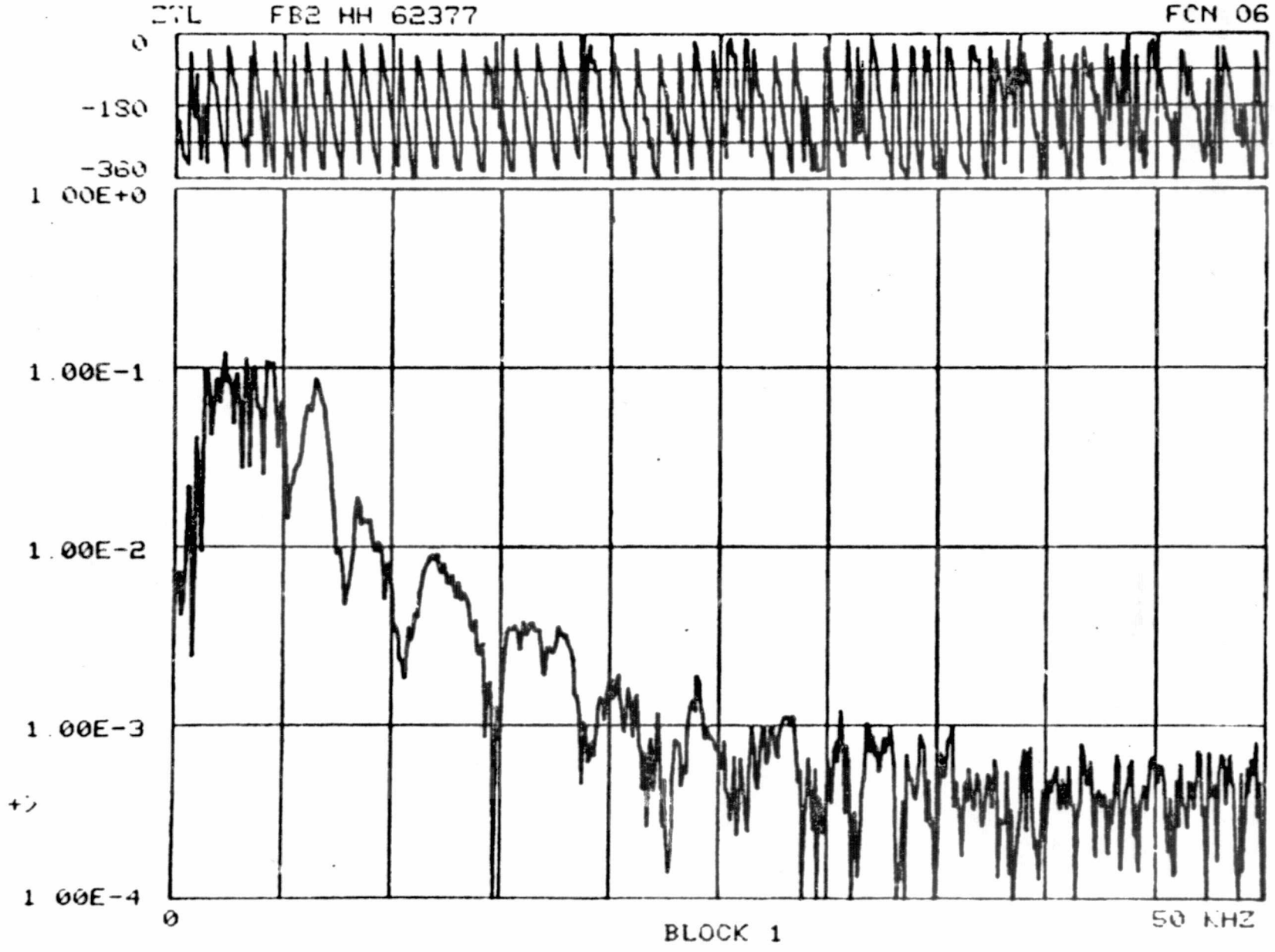
FB2 HH 62377
FCN 06
0
-180
-360
1.00E+0
1.00E-1
1.00E-2
1.00E-3
1.00E-4
0
50 KHZ
BLOCK 1

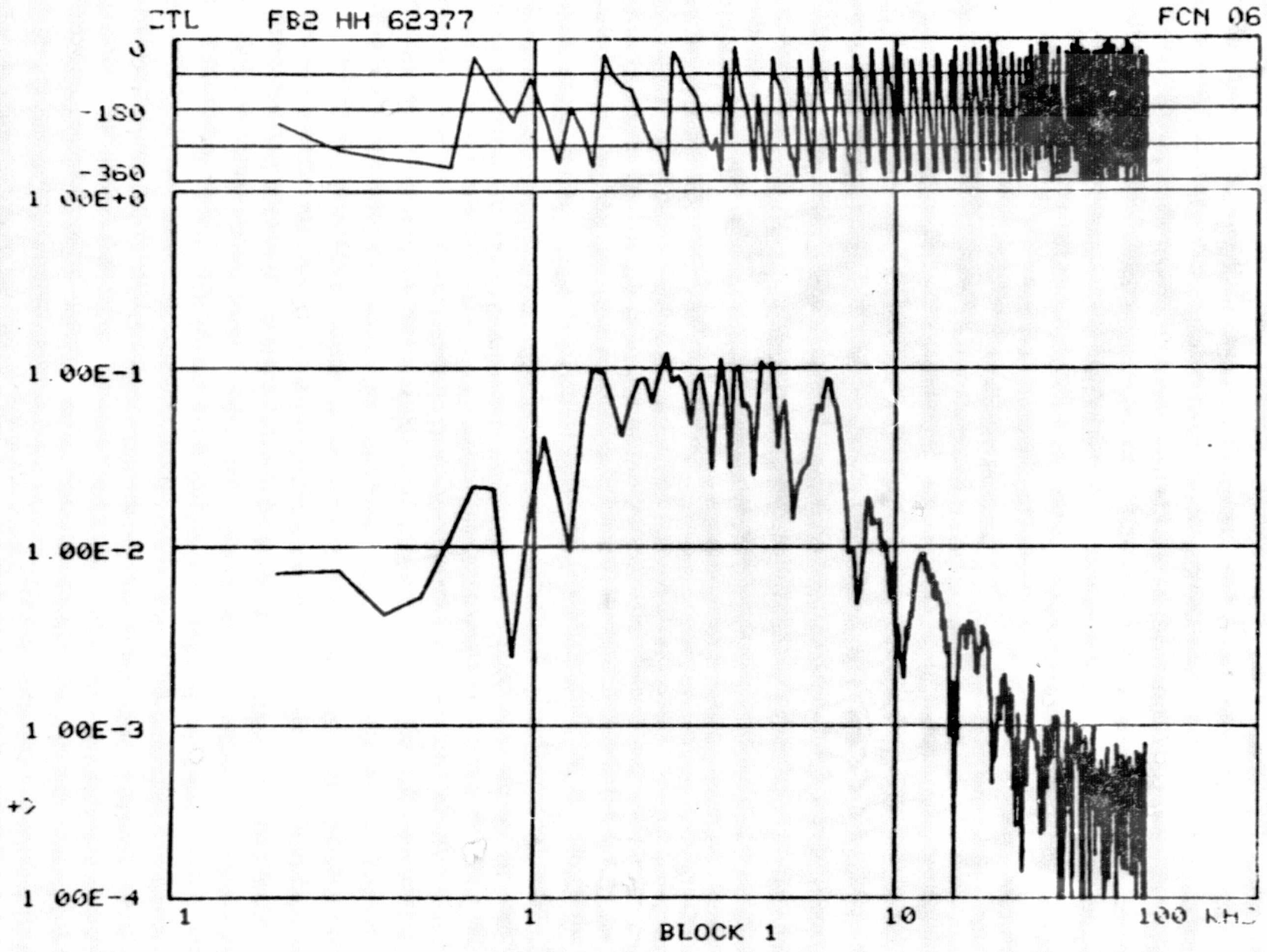
CTL FB2 HH 62377
FCN 06
0
-180
-360
1.00E+0
1.00E-1
1.00E-2
1.00E-3
1.00E-4
1
1
10
100 KHZ
BLOCK 1

```
+   FEB HH 82377
+
+   ? 6
START FREQ    ? 10
END FREQ      ? 15000
SEARCH DISPLAY #? 1
# PEAKS? 16

RANK    CHANNEL NO.     FREQUENCY     F1(N)        F2(N)
1               24       2.34E+3     1.20E-1    -3.43E+2
2               34       3.32E+3     1.11E-1    -3.27E+2
3               44       4.29E+3     1.06E-1    -2.31E+2
4               47       4.58E+3     1.05E-1    -4.17E+1
5               38       3.71E+3     1.00E-1    -9.55E+1
6               15       1.46E+3     9.60E-2    -3.18E+2
7               30       2.92E+3     9.12E-2    -2.09E+2
8               26       2.53E+3     8.91E-2    -5.91E+1
9               21       2.05E+3     8.58E-2    -2.31E+2
10              67       6.54E+3     8.52E-2    -2.33E+2
11              51       4.98E+3     6.50E-2    -1.85E+2
12              40       3.90E+3     6.25E-2    -1.69E+2
13              63       6.15E+3     6.11E-2    -6.65E+1
14              11       1.07E+3     4.10E-2    -2.00E+2
15               7       6.82E+2     2.15E-2    -4.23E+1
16              87       8.49E+3     1.83E-2    -3.19E+2
+>
```

FCN 01

CTL FB4 62377

CTL FB4 62377

FCN 0

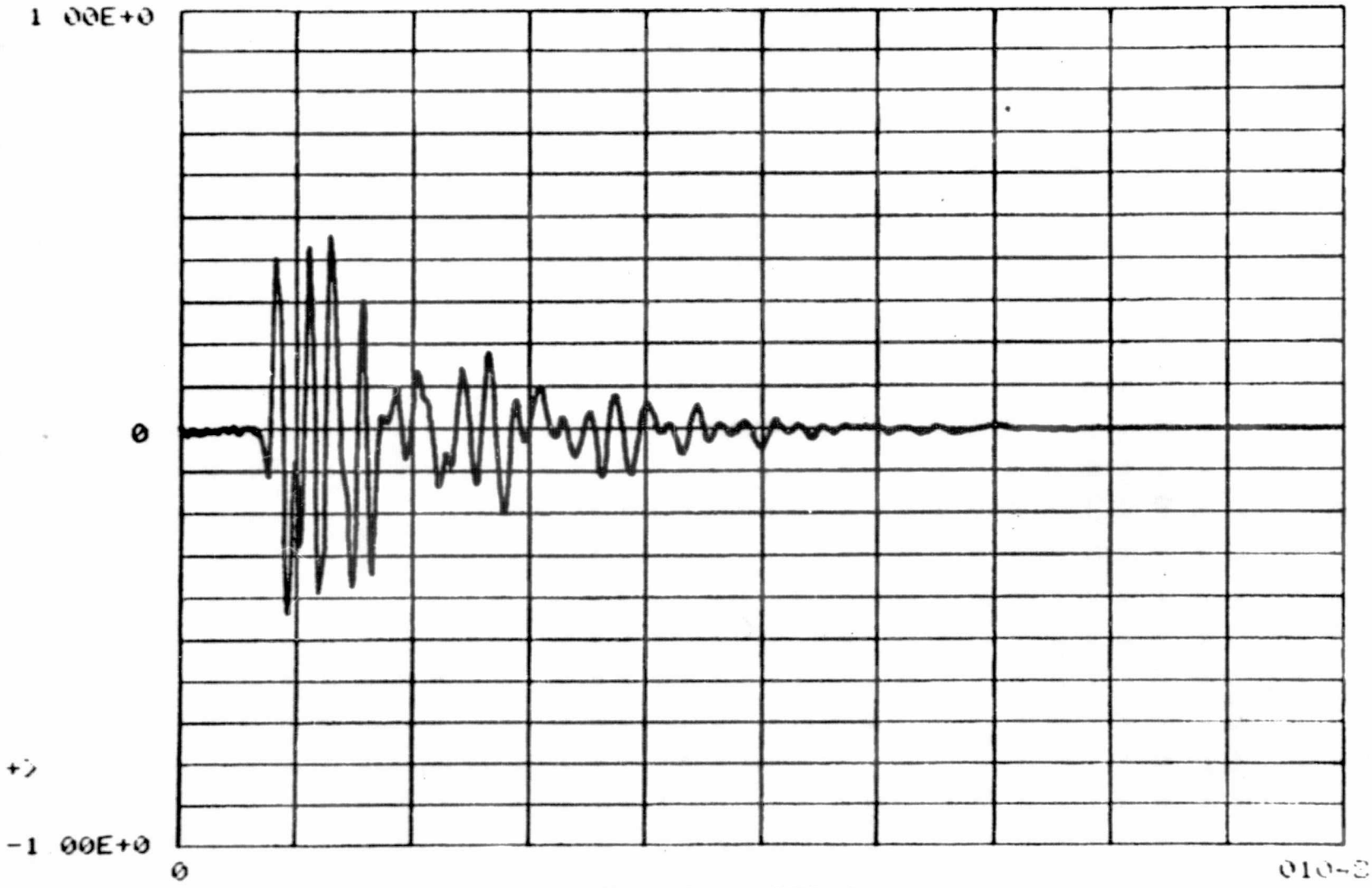

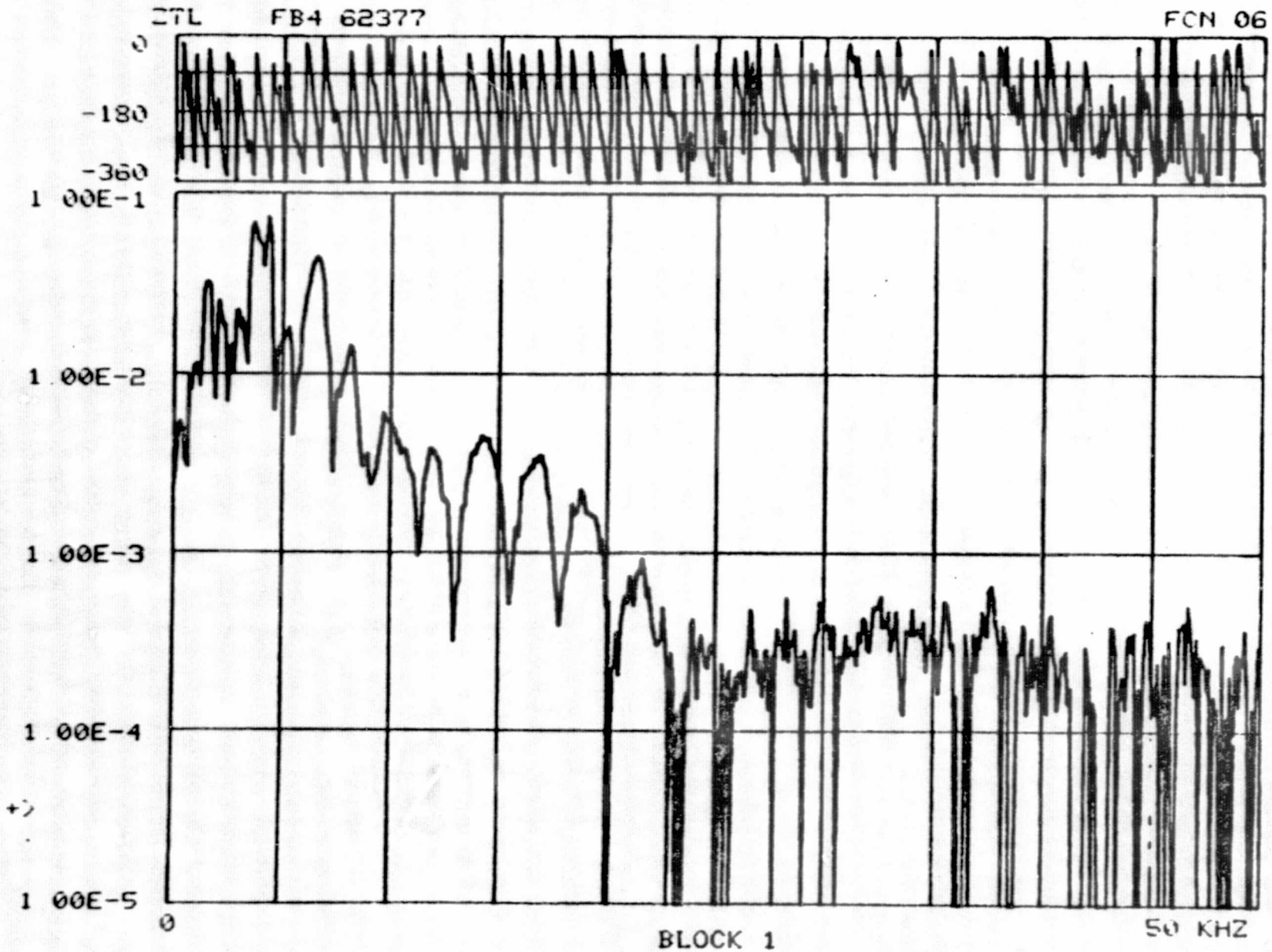
ITL
FB4 62377
FCN 06
0
-180
-360
1 00E-1
1 00E-2
1 00E-3
1 00E-4
1 00E-5
0
BLOCK 1
50 KHZ

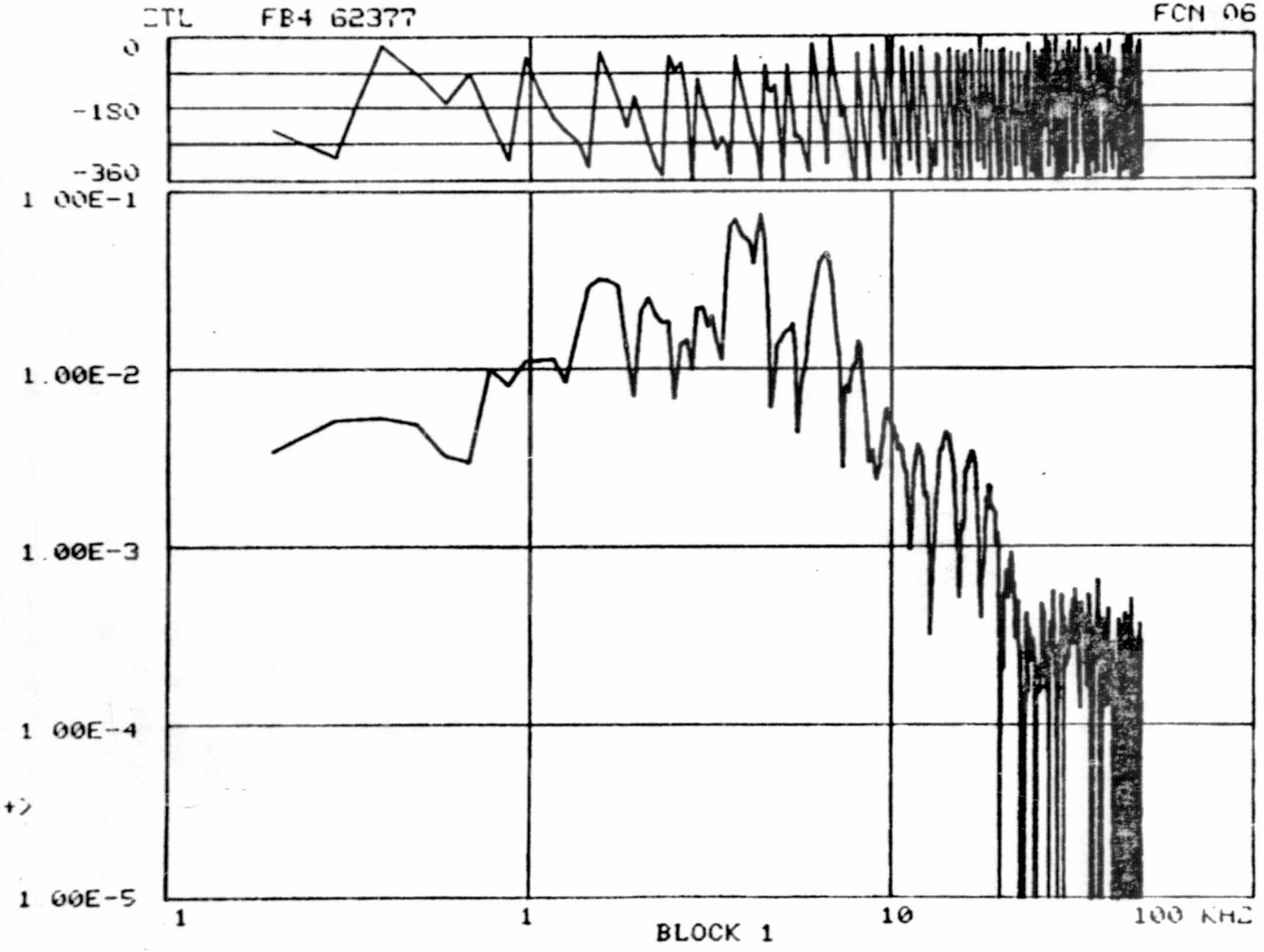
CTL
FB4 62377
FCN 06
0
-180
-360
1.00E-1
1.00E-2
1.00E-3
1.00E-4
1.00E-5
+)
1
1
10
100 KHZ
BLOCK 1

```
+>   FB4 HH 62377
+>
+>   ? 6
START FREQ    ? 10
END FREQ    ? 15000
SEARCH DISPLAY #? 1
# PEAKS? 16

RANK    CHANNEL NO.      FREQUENCY     F1(N)        F2(N)
1                45       4.39E+3     7.33E-2    -3.49E+2
2                38       3.71E+3     6.87E-2    -4.19E+1
3                68       6.64E+3     4.39E-2    -2.69E+2
4                16       1.56E+3     3.17E-2    -3.32E+1
5                22       2.14E+3     2.50E-2    -2.65E+2
6                31       3.02E+3     2.19E-2    -1.69E+2
7                33       3.22E+3     2.01E-2    -2.39E+2
8                25       2.44E+3     1.85E-2    -4.18E+1
9                55       5.37E+3     1.81E-2    -1.85E+2
10               28       2.73E+3     1.42E-2    -1.61E+2
11               84       8.20E+3     1.41E-2    -8.81E+1
12               12       1.17E+3     1.13E-2    -2.04E+2
13               8        7.81E+2     9.88E-3    -2.10E+2
14               78       7.61E+3     8.13E-3    -2.39E+2
15               100      9.76E+3     6.00E-3    -1.40E+0
16               4        3.90E+2     5.31E-3    -1.81E+1
+>
```

ZTL FB5 62377 FCN 01

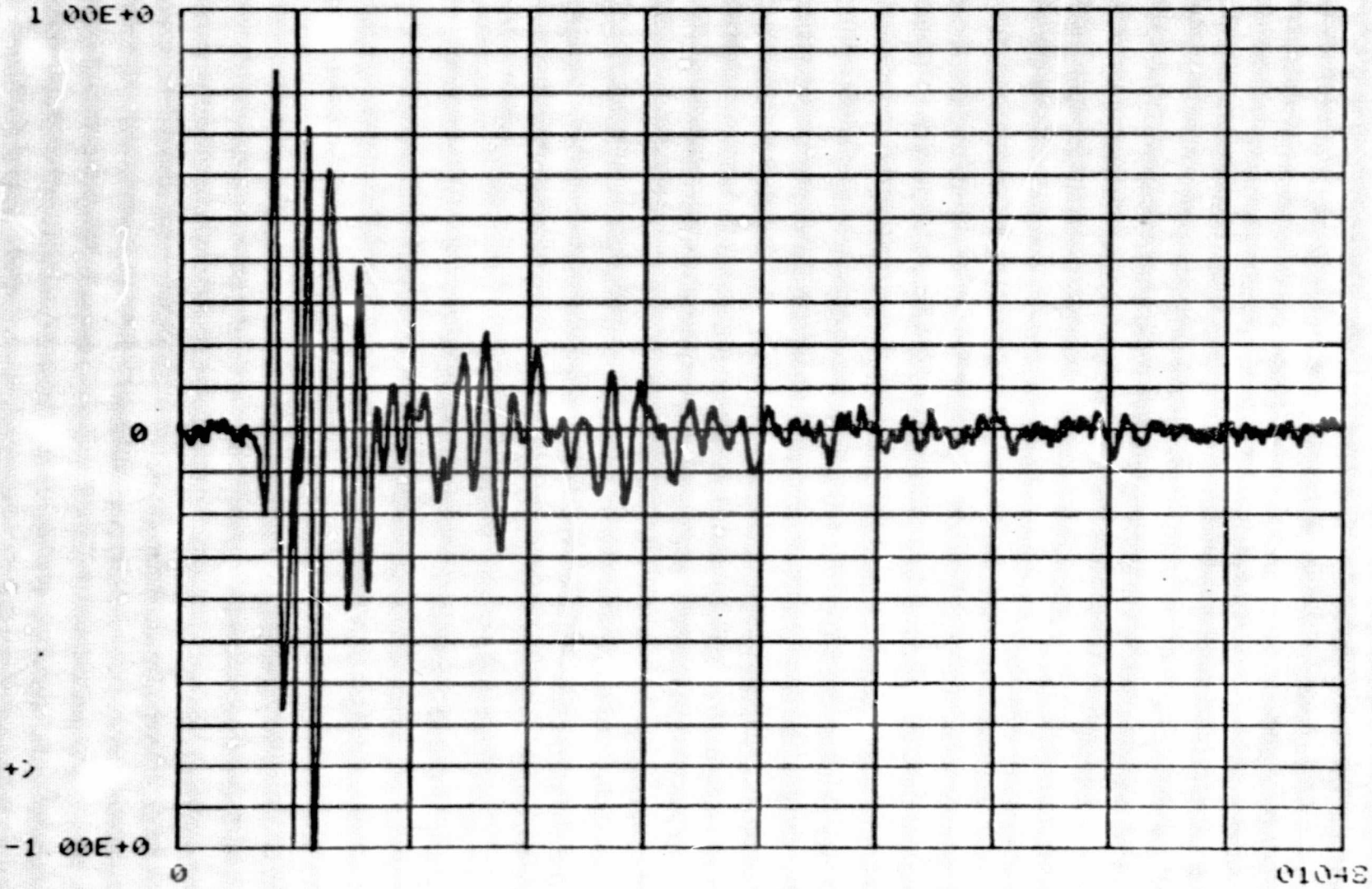

CTL FBS HH 62377 FCN 0

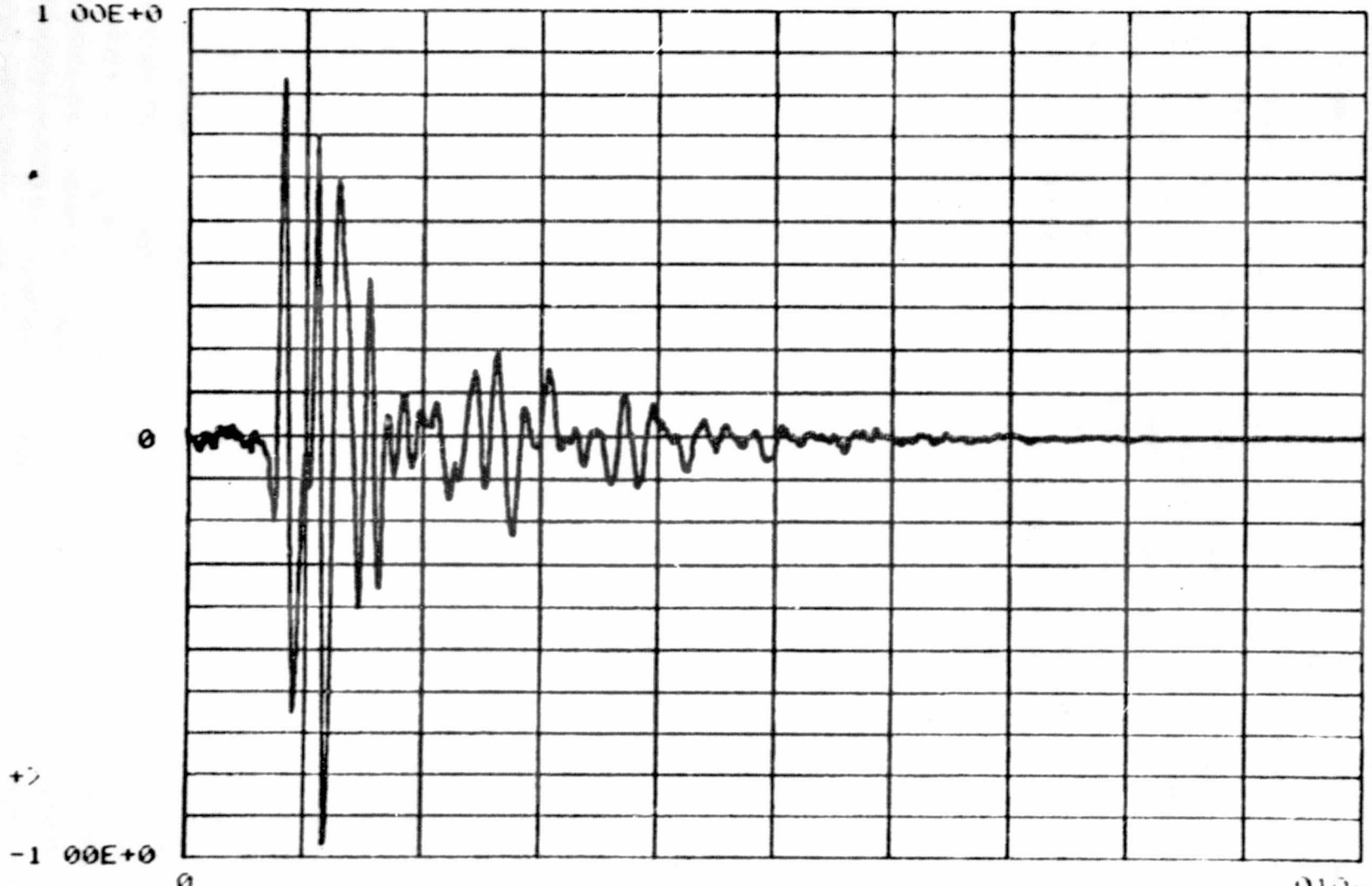

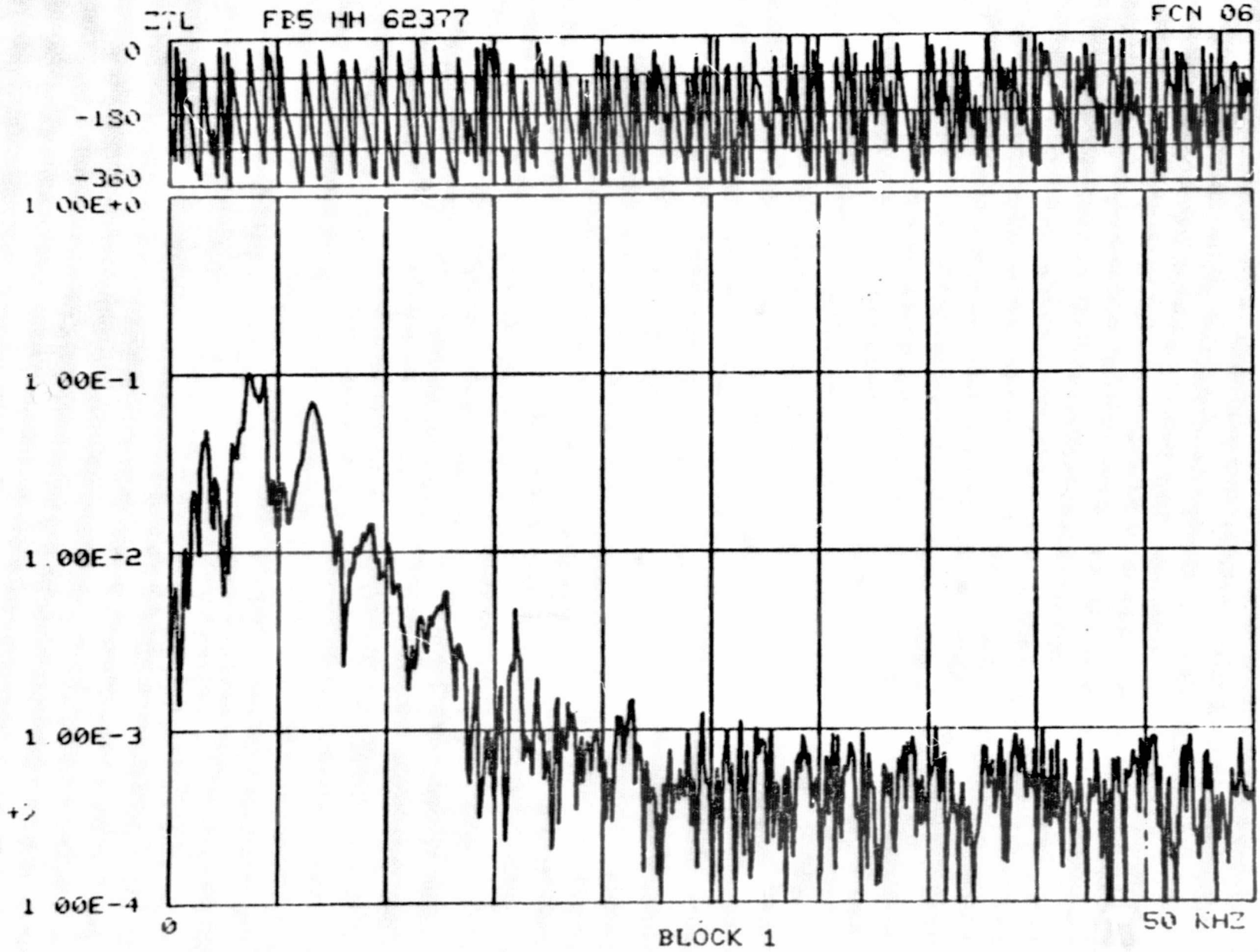
ITL FBS HH 62377
FCN 06
0
-180
-360
1.00E+0
1.00E-1
1.00E-2
1.00E-3
1.00E-4
0
50 KHZ
BLOCK 1

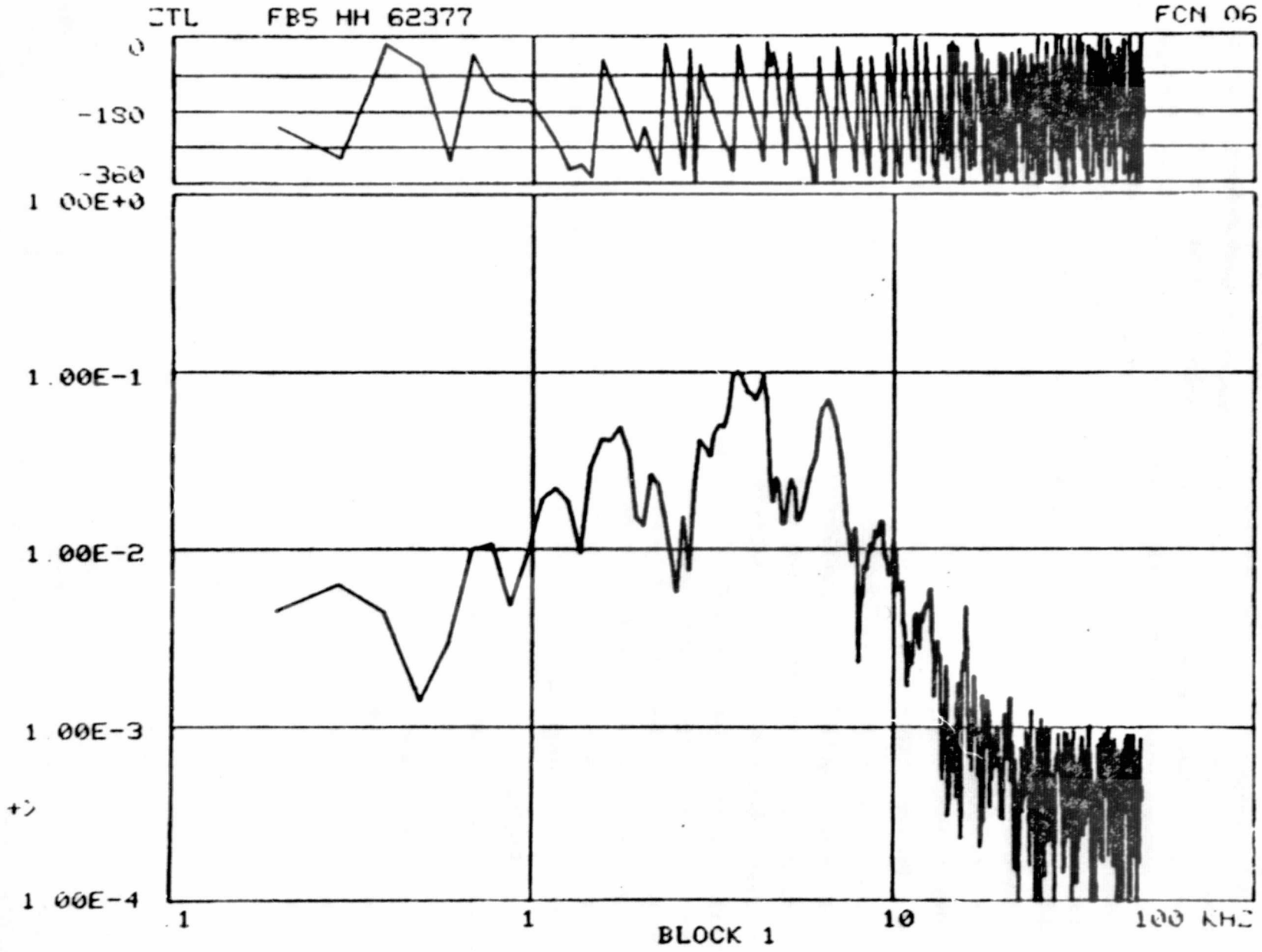
CTL FBS HH 62377
FCN 06
0
-180
-360
1.00E+0
1.00E-1
1.00E-2
1.00E-3
1.00E-4
1
1
10
100 KHZ
BLOCK 1

```
+)  FBS HH 62377

+)  ? 6
START FREQ    ? 10
END FREQ    ? 15000
SEARCH DISPLAY #? 1
# PEAKS? 16

RANK    CHANNEL NO.     FREQUENCY     F1(N)        F2(N)
1               38       3.71E+3     1.01E-1    -1.87E+1
2               45       4.39E+3     9.50E-2    -3.03E+2
3               68       6.64E+3     6.83E-2    -2.14E+2
4               34       3.32E+3     4.97E-2    -2.24E+2
5               18       1.75E+3     4.80E-2    -1.62E+2
6               16       1.56E+3     4.17E-2    -5.31E+1
7               30       2.92E+3     4.10E-2    -6.52E+1
8               22       2.14E+3     2.60E-2    -2.76E+2
9               49       4.78E+3     2.52E-2    -7.91E+1
10              54       5.27E+3     2.44E-2    -1.01E+2
11              12       1.17E+3     2.20E-2    -2.57E+2
12              27       2.63E+3     1.48E-2    -3.23E+2
13              96       9.37E+3     1.40E-2    -2.94E+2
14              81       7.91E+3     1.29E-2    -3.29E+2
15              92       8.98E+3     1.25E-2    -1.53E+2
16             104       1.01E+4     1.09E-2    -2.13E+2
+)
```

CTL MCP 62377 FCN 01

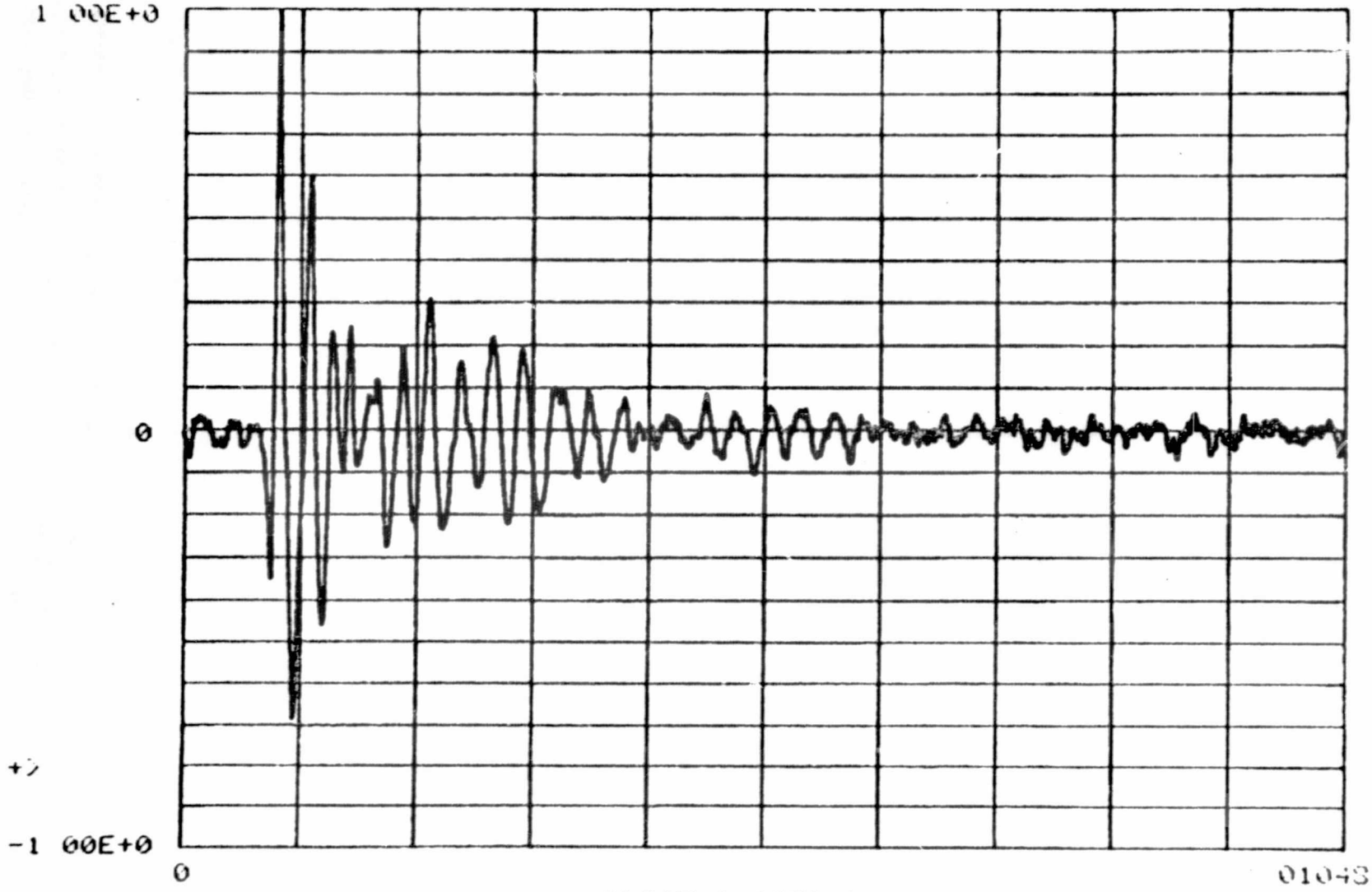

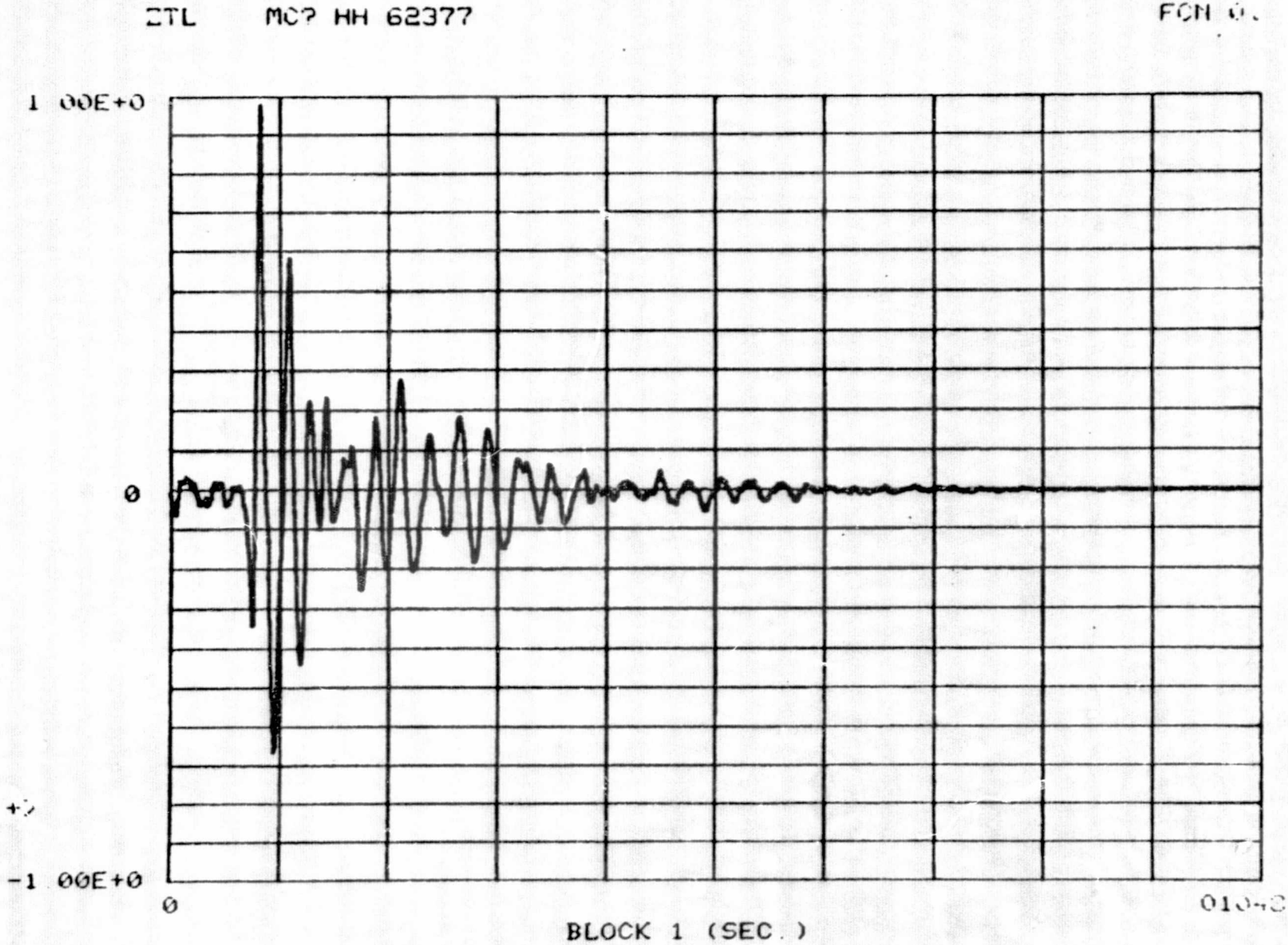
ZTL MC? HH 62377
FCN 0.
1.00E+0
0
-1.00E+0
0
BLOCK 1 (SEC.)

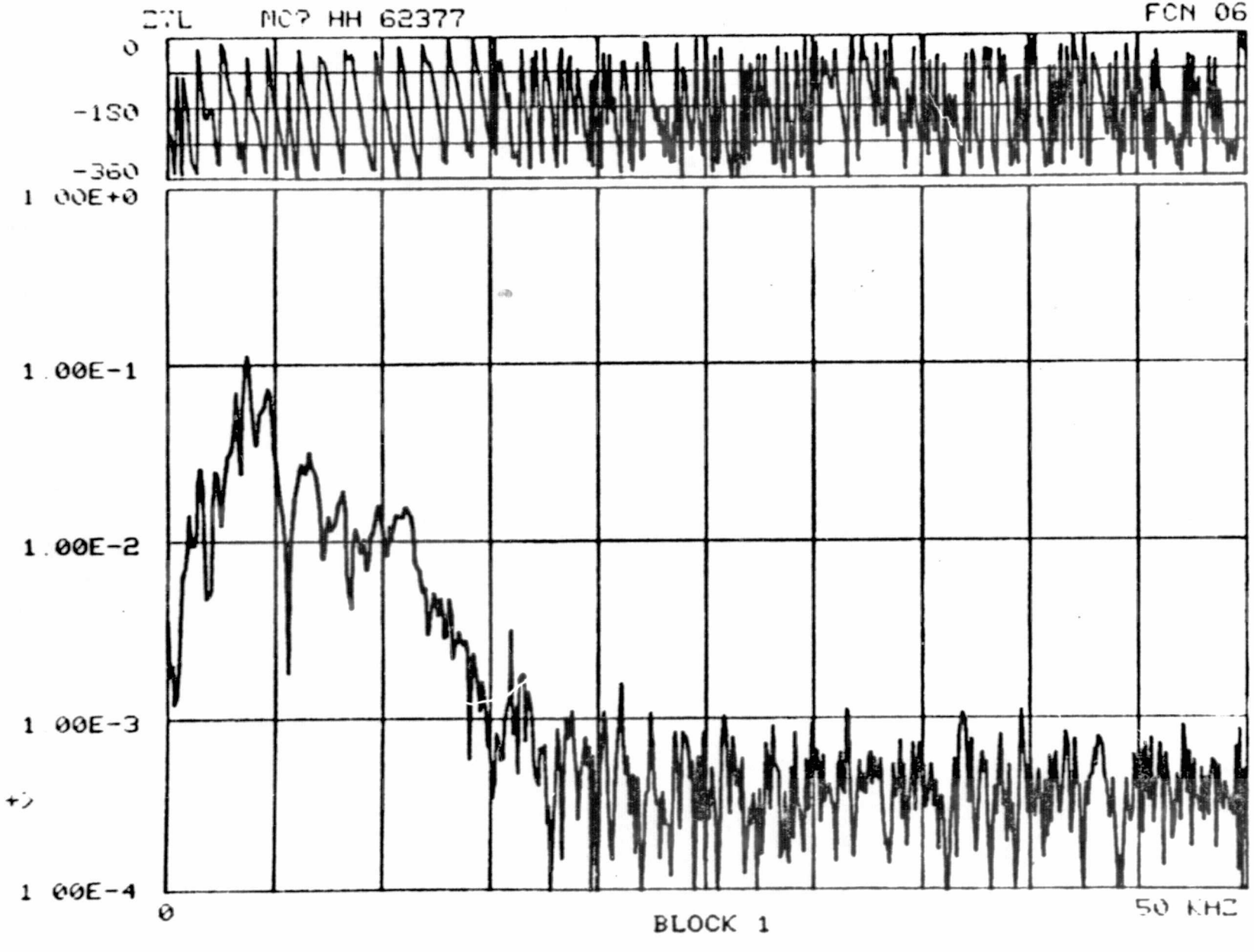

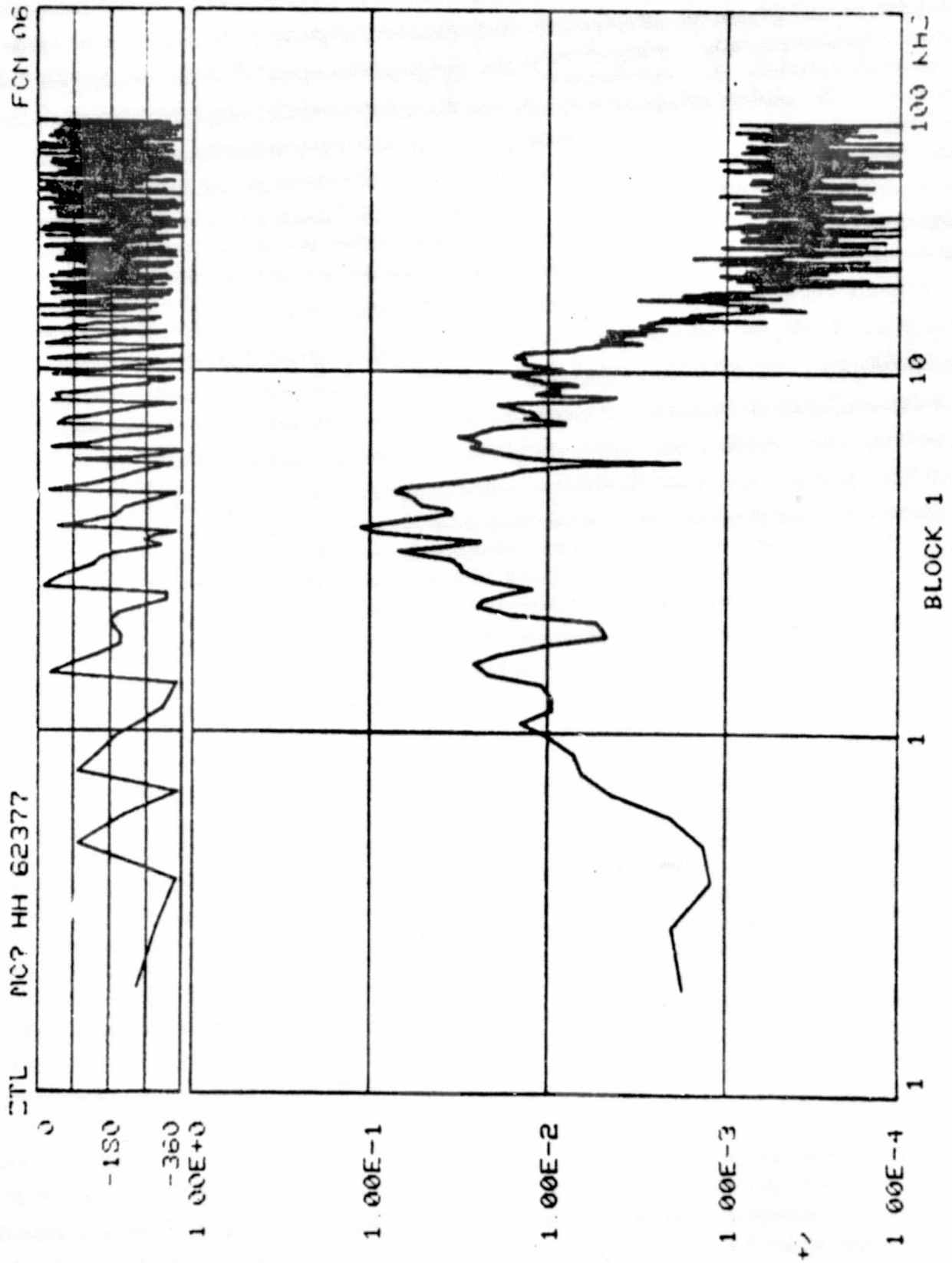
FCN 06
ETL MC2 HH 62377
0
-180
-360
1.00E+0
1.00E-1
1.00E-2
1.00E-3
1.00E-4
1
10
100 KHz
BLOCK 1

```
+)   MC? HH 62377
+)
+)   ? 6
START FREQ    ? 10
END FREQ.   ? 15000
SEARCH DISPLAY #? 1
# PEAKS? 16

RANK    CHANNEL NO.      FREQUENCY     F1(N)        F2(N)
1               38        3.71E+3     1.10E-1    -4.89E+1
2               48        4.68E+3     7.22E-2    -2.41E+1
3               33        3.22E+3     6.85E-2    -2.42E+2
4               68        6.64E+3     3.17E-2    -2.27E+2
5               64        6.25E+3     2.69E-2    -7.47E+1
6               16        1.56E+3     2.55E-2    -9.53E+1
7               23        2.24E+3     2.45E-2    -2.61E+2
8               84        8.20E+3     1.88E-2    -3.39E+2
9              101        9.86E+3     1.56E-2    -7.62E+1
10             114        1.11E+4     1.51E-2    -1.27E+2
11              11        1.07E+3     1.40E-2    -2.56E+2
12             109        1.06E+4     1.38E-2    -3.17E+2
13             111        1.08E+4     1.36E-2    -2.28E+1
14              77        7.51E+3     1.34E-2    -1.17E+2
15             106        1.03E+4     1.19E-2    -2.16E+2
16              90        8.78E+3     1.16E-2    -1.04E+2
+>
```

APPENDIX B

Acoustic emission data was obtained some time ago from a number of compressive tests performed on boron-aluminum reinforced titanium hat-stiffeners fabricated by different techniques. This data was analyzed by usual AE count rate and total count curves and reported in "Acoustic Emission Characterization of Compressive Failures of Composite Stiffeners," Final Report for NASA Contract NAS1-13175-Task 12, November, 1975, by Edmund G. Henneke, (Virginia Tech, College of Engineering Report No. VPI-E-75-24). This data has been analyzed by the new FFT system and is reported here. For these tests, the acoustic emission signals were averaged for the entire test run and the frequency spectrum of the average signal is reported here as an auto spectrum. The scale factor for these plots is X2, i.e., the true frequencies are twice those shown on the horizontal scale. For these plots, the frequency data is therefore significant up to only 75 KHz on the graphs (150 KHz true frequency).

The frequency auto spectra associated with each type of specimen are quite distinctive as one can see after some study of the plots. The specimens were geometrically similar for each type but the boron-aluminum stiffeners were bonded to the hats differently. This could account for the different frequency response. On the other hand, it may also be due to different failure mechanisms exciting the hats differently as indicated in the text.

ZTL SPEC D-5

FCN 23

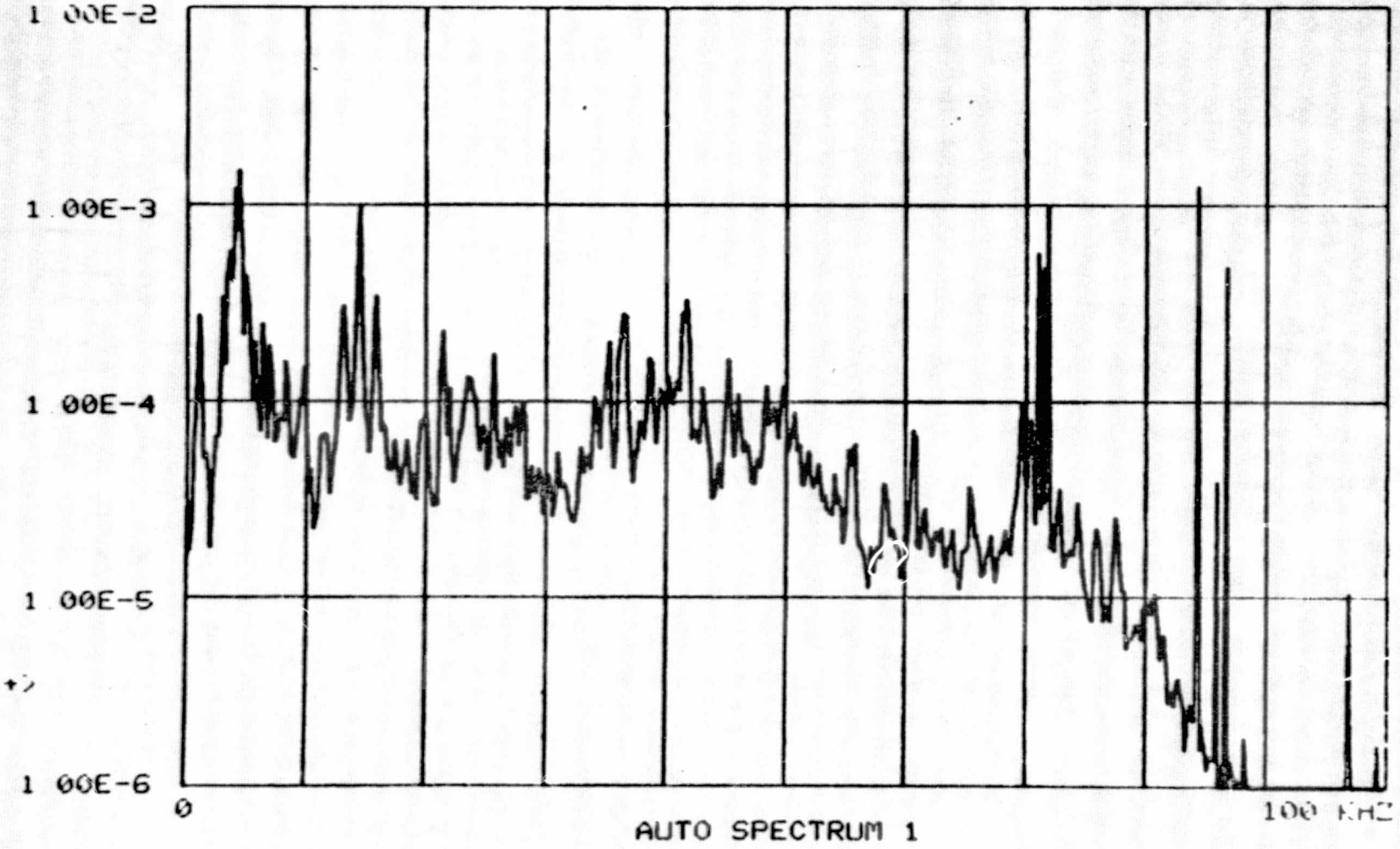

ZTL SPEC D-15 FCN 23

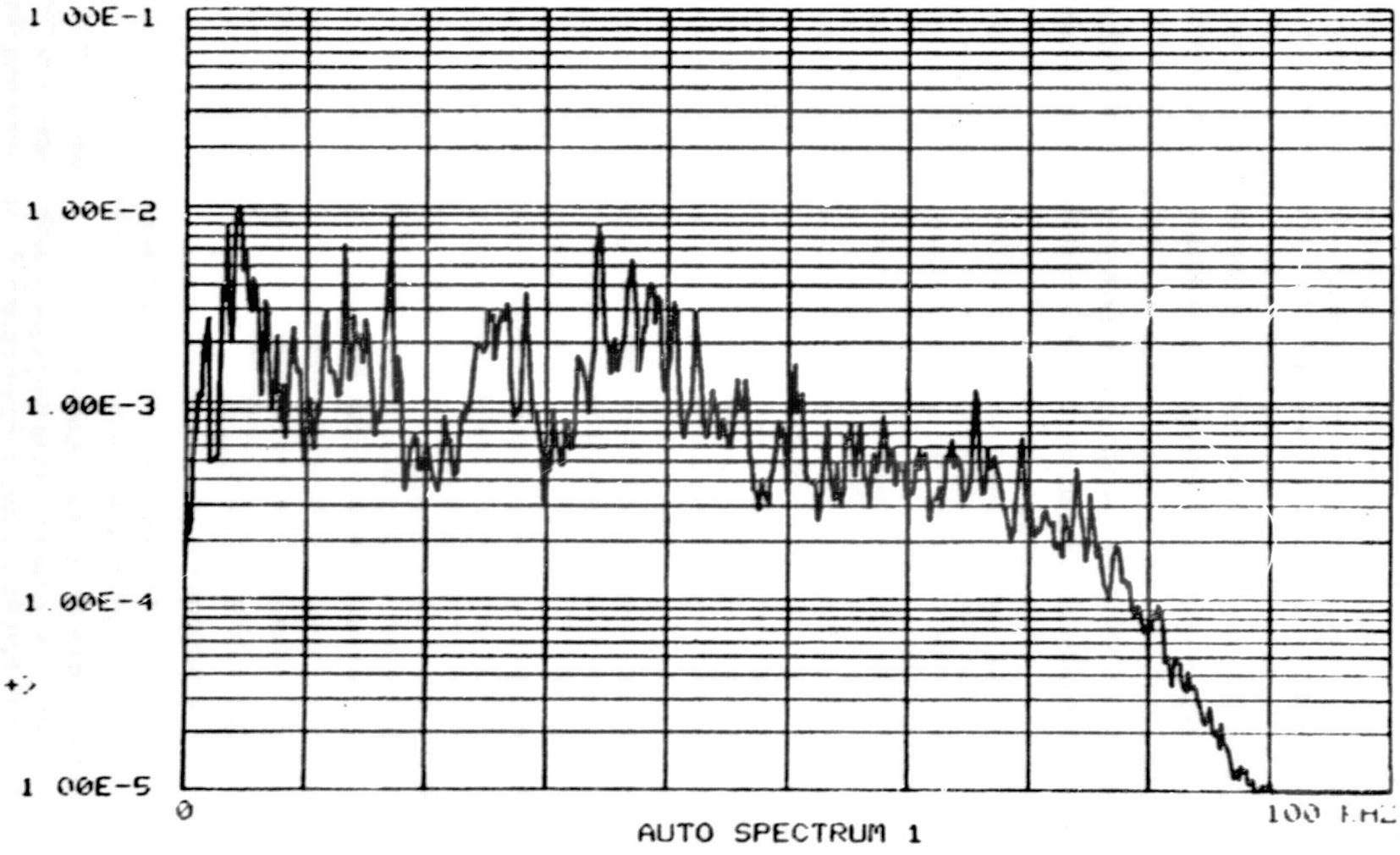

CTL SPEC A-45 FCN 20

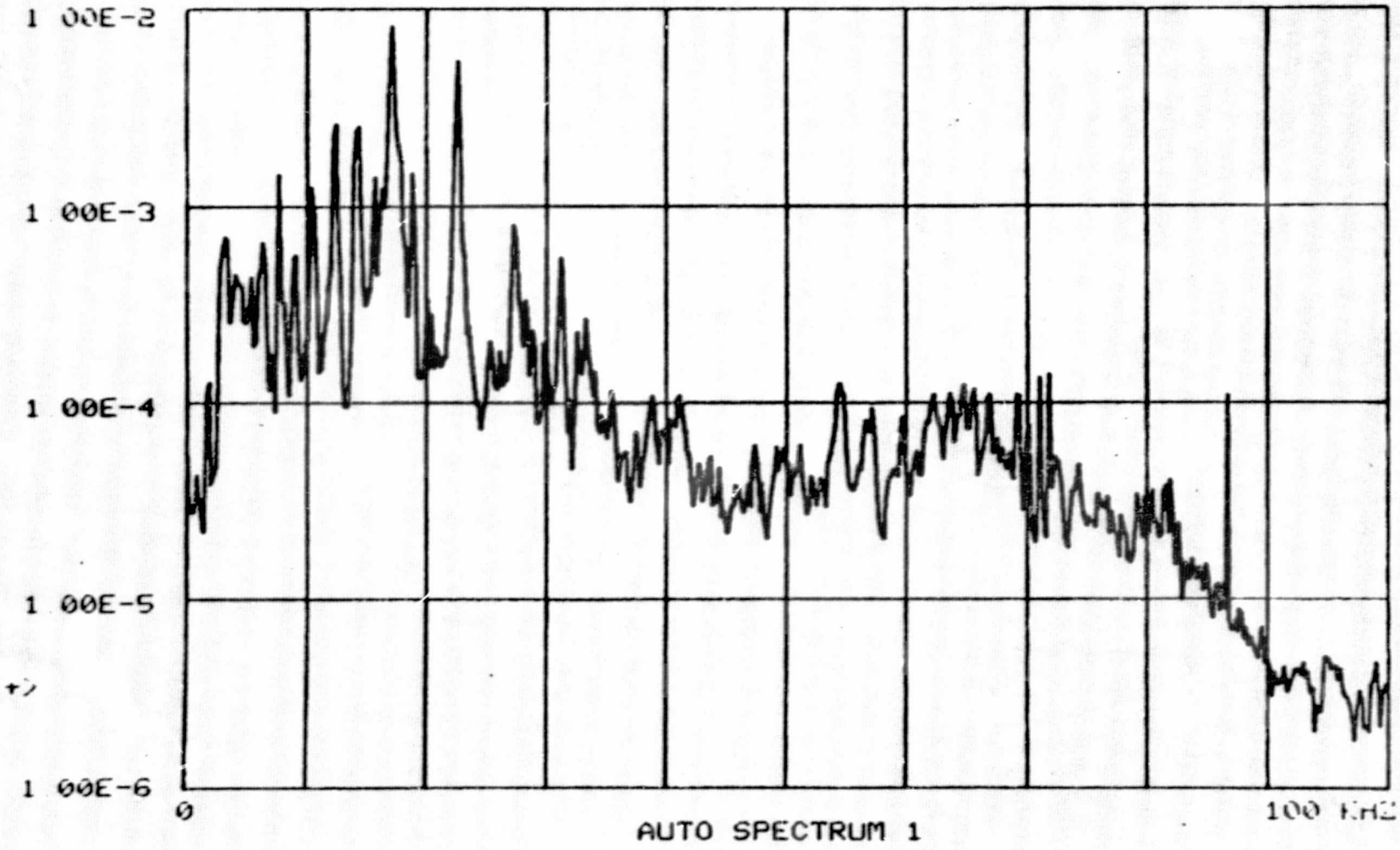

ITL SPEC A-15 FCN 23

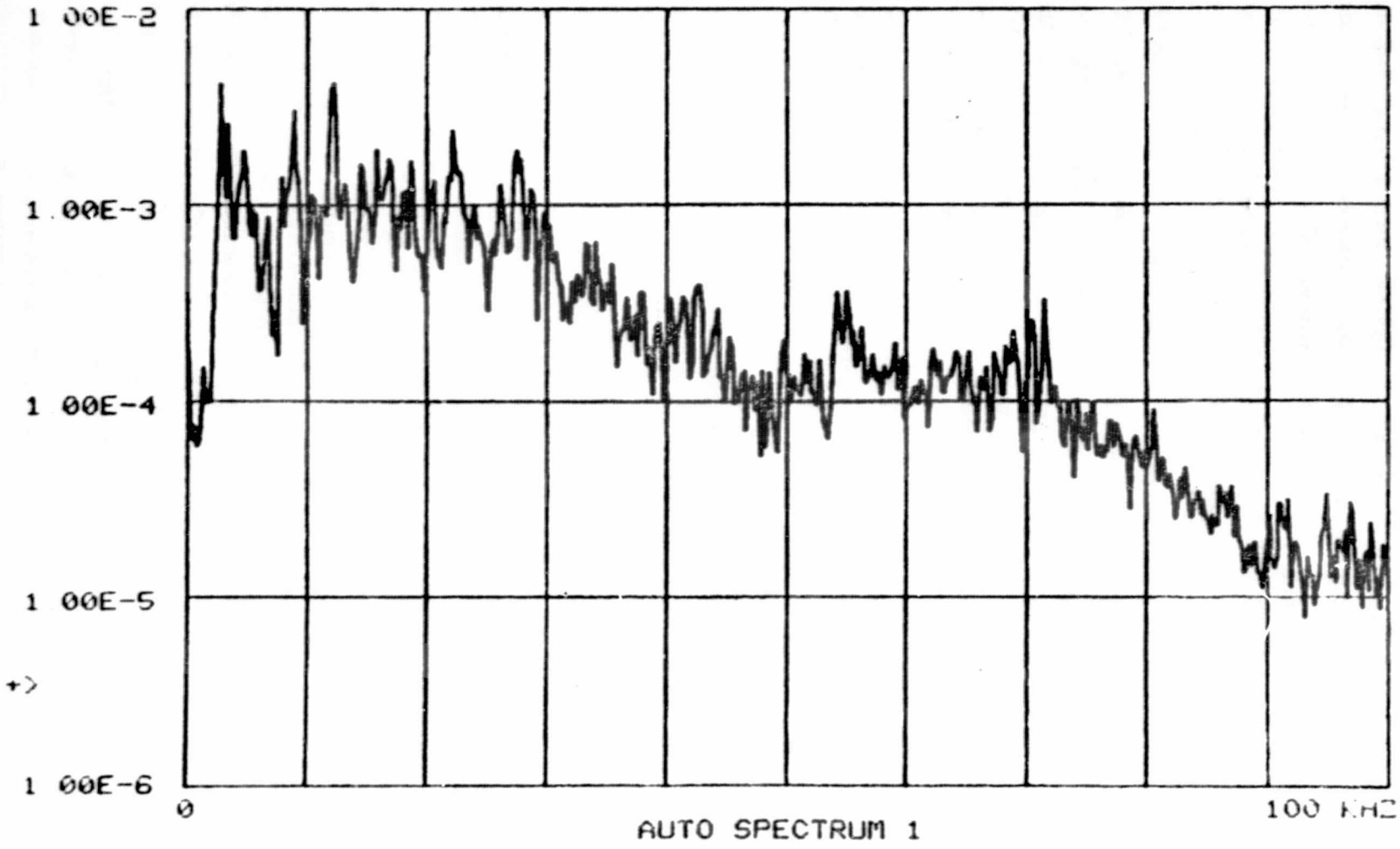

CTL SPEC F-9 FCN 33

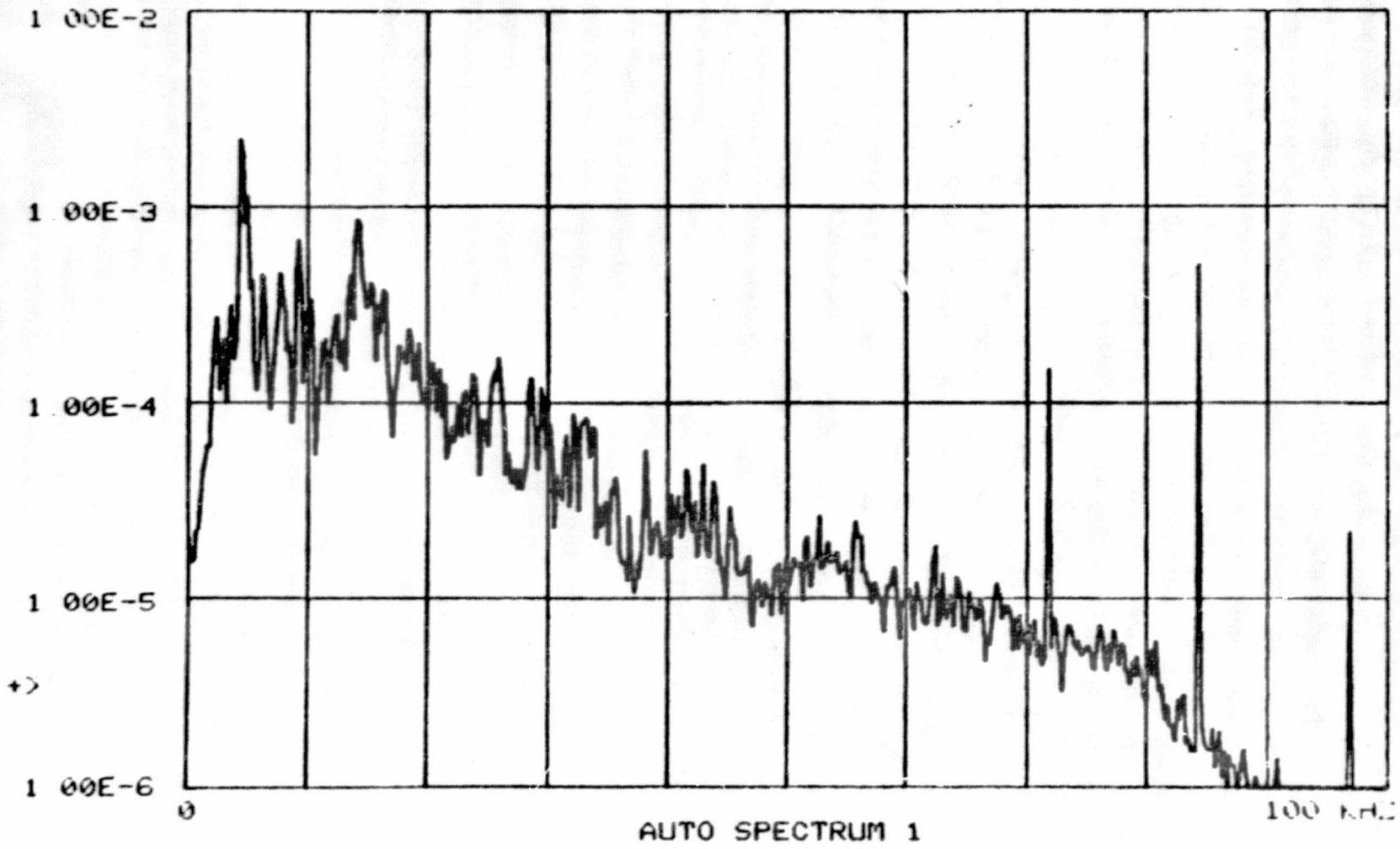

CTL SPEC F-59 FCN 23